February 2020
Ph.D. Dissertation

Low density lipoprotein receptor-related protein 5 regulates HIF-1α stability in ischemic myocardium via the interaction with PHD2

Graduate School of Chosun University

Department of Biomedical Sciences

Sujin Ju

Low density lipoprotein receptor-related protein 5 regulates HIF-1α stability in ischemic myocardium via the interaction with PHD2

허혈성 심장질환에서 LRP5 의 PHD2 와의 결합을 통한
HIF-1α 안정성 조절 기전 규명

25th February 2020

Graduate School of Chosun University

Department of Biomedical Sciences

Sujin Ju

Low density lipoprotein receptor-related protein 5 regulates HIF-1α stability in ischemic myocardium via the interaction with PHD2

Advisor: Prof. Heesang Song

This dissertation is submitted to the Graduate School of Chosun University in partial fulfillment of the requirements for the degree of Doctor of Philosophy

October 2019

Graduate School of Chosun University

Department of Biomedical Sciences

Sujin Ju

This certifies that the Doctoral Dissertation of Sujin Ju is approved.

Chairman: Chosun Univ., Prof. Byoung Rai Lee .....

Member: Chosun Univ., Prof. Ho Jin You .....

Member: Nambu Univ., Prof. Young-Beob Yu .....

Member: Korea Univ., Prof. In-Geol Choi .....

Member: Chosun Univ., Prof. Heesang Song .....

December 2019

Graduate School of Chosun University

CONTENTS

Abbreviations

CAD	Coronary artery disease
MI	Myocardial infarction
LRP5	Low-density lipoprotein receptor-related protein 5
LRP6	Low-density lipoprotein receptor-related protein 6
EGF	Epidermal growth factor
DKK1	Dickkopf1
Mesd	Mesoderm development
CK1	Casein kinase 1
GSK3	Glycogen synthase kinase-3
KLF15	Krüppel-like factor 15
Sp1	Specificity protein 1
PKA	Protein kinase A
TPH1	Tryptophan hydroxylase 1
OPPG	Osteoporosis pseudoglioma
SCID	Severe combined immunodeficient mice
HBM	High-bone-mass
PC	Prostate cancer
OS	Osteosarcoma
APOE	Apolipoprotein E
HIF-1α	Hypoxia inducible factor-1α
PHD	Prolyl hydroxylases
pVHL	Von Hippel-Lindau protein
FIH	Factor inhibiting HIF
HRE	Hypoxia-response elements

ROS	Reactive oxygen species
DMOG	Dimethyloxallyl glycine
I/R	Ischemia/reperfusion
Cx43	Connexin 43
EPO	Erythropoietin
NOS2	Nitric oxide synthase 2
PFKFB3	6-Phosphofructo-2-Kinase/Fructose-2,6-Biphosphatase 3
BNIP3L	BCL2 interacting protein 3 like
GLUT-1	Glucose transporter 1
CHX	Cycloheximide

List of Tables

List of Figures

Abstract

Low density lipoprotein receptor-related protein 5 regulates HIF-1αstability in ischemic myocardium via the interaction with PHD2

Sujin Ju

Advisor: Prof. Heesang Song, Ph.D.

Department of Biomedical Sciences

Graduate School of Chosun University

Hypoxia is associated with various pathologic conditions including myocardial infarction (MI). Despite improvements in the diagnosis and treatment for cardiac pathologies, MI remains the leading cause of death and disability worldwide. The transcription factor hypoxia inducible factor-1α (HIF-1α) plays a crucial role in acute hypoxic responses by activating the transcriptional target genes involved in glycolysis, erythropoiesis and survival. Therefore, activation of HIF-1α in ischemic hearts has been considered a target for therapeutic strategies. Here, this study identified that LRP5 is a novel negative regulator of HIF-1α stability in ischemic myocardium.

Low-density lipoprotein receptor-related protein 5 (LRP5) belongs to the LDLR family and functions as an essential co-receptor for Wnt/β-catenin signaling activation. Although inhibition of Wnt/β-catenin signaling has been

reported to protect myocardial death against ischemia/reperfusion (I/R) injury, there is little understanding on the role of LRP5 in ischemic myocardium. Therefore, the aim of this study was to investigate the functions of LRP5 in hypoxia-induced cardiomyocytes in *in vitro* and *in vivo*. Exposure to acute hypoxia (O_2 1.2%) in cardiomyocytes increased the expression of LRP5, whereas the expression of LRP6 decreased. The MTT and trypan blue staining assay revealed that silencing of LRP5 highly increased the survival rates of cardiomyocytes under hypoxic condition. In contrast, silencing of LRP6 more inhibited cell viability, indicating that LRP5 and LRP6 display converse function against hypoxia-induced cardiomyocytes death. Significant reductions of Annexin V-positive cells, caspase-3 activation and Bax/Bcl-2 ratio were observed in LRP5 silenced and LRP6 overexpressed-hypoxic cardiomyocytes. In contrast, LRP5 overexpression and LRP6 silencing increased Annexin V-positive cells, caspase-3 activation and Bax/Bcl-2 ratio under hypoxic conditions. Gene expression analysis (mRNA-seq) and qPCR results demonstrated that the transcriptional activity of HIF-1α target genes were strongly reduced when LRP5 was overexpressed in hypoxic cardiomyocytes, whereas they were markedly upregulated by silencing of LRP5. Overexpression of LRP5 aggravated HIF-1α stability through the ubiquitin-proteasomal pathway under hypoxc conditions. Furthermore, this study showed that LRP5 regualtes hydroxylation of HIF-1α at the oxygen-dependent degradation domain (ODDD) mediated by interacting with PHD2. Interestingly, LRP6 did not interact with PHD2. This study further identified the phosphorylation of LRP5 is responsible for HIF-1α degradation and which is independent of Wnt/β-catenin signaling pathway. Consistently, direct myocardial delivery of adenoviral constructs for either overexpression or silencing of LRP5 in *in vivo* showed silencing of LRP5 significantly improved

cardiac function against myocardial infarction model. Together, these results demonstrated unknown role of LRP5 as a regulator of HIF-1a stability in myocardial infarction, which is provided potential value as a new target for ischemic injury treatment.

초록

허혈성 심장질환에서 LRP5 의 PHD2 와의 결합을 통한 HIF-1α 안정성 조절 기전 규명

주 수 진

지도교수: 송 희 상

의과학과

조선대학교 대학원

저산소증은 심근경색과 같은 다양한 병리학적 질환과 관련이 있다. 심근경색증은 대표적인 허혈성 심장질환으로 진단과 치료의 개선에도 불구하고, 여전히 전세계적으로 높은 사망률과 장애를 유발하는 주요원인으로 알려져 있다. 저산소 유도인자인 HIF-1α는 저산소상태에서 외부위 산소 농도 변화에 적절하게 반응하기 위해 해당과정, 적혈구생성 및 생존과 관련된 유전자의 발현을 유도함으로서 세포내의 항상성을 유지시켜주는 전사인자로 중요한 역할을 한다. 따라서, 허혈성 심근경색의 치료 표적으로 HIF-1α 의 활성과 발현 증진 조절을 위한 기전 연구와 활성화 가능 약물 개발 연구가 다양하게 이루어지고 있다. 본 연구에서는 LRP5 라는 수용체

단백질이 저산소가 유도된 심근에서 HIF-1α의 안정성을 조절하는 새로운 타겟이 될 수 있다는 것을 확인하였다.

저밀도 지단백 관련 단백질 5 (LRP5)는 LDLR family 에 속하는 수용체로로서, LRP6 와 함께 Wnt/β-catenin 신호경로를 활성화시키기 위한 co-receptor 로서 기능을 한다. 비록 Wnt/β-catenin 신호 억제가 저산소/재관류 유도된 심근 손상을 보호하는 것으로 보고되었지만, 허혈성 심근에서 LRP5 의 역할 및 관련 기전에 대한 이해가 부족하였다. 따라서, 본 연구의 목적은 저산소가 유도된 심근세포에서 LRP5 의 기능을 *in vitro* 와 *in vivo* 에서 조사하는 것이었다. 급성 저산소증 (O_2 1.2%)에 노출된 심근세포에 LRP5 의 발현이 증가되는 반면, LRP6 의 발현은 감소하였다. MTT 와 Trypan blue staining assay 을 통해 LRP5 의 저해는 대조군과 비교하여 저산소로 유도된 심근세포의 생존율을 크게 증가시키고, 반대로 LRP6 의 저해는 심근세포의 사멸을 더욱 촉진시키는 것을 확인하였다. 이러한 결과는, LRP5 와 LRP6 가 저산소 유도된 심근세포의 사멸에 있어서 반대되는 역할을 기여하는 것으로 사료된다. LRP5 의 저해 및 LRP6 가 과발현된 심근세포는 저산소에 의해 유도된 Annexin-V 양성세포, caspase-3 의 활성화 및 Bax/Bcl-2 비율을 유의미하게 감소시켰다. 이와는 대조적으로, LRP5 의 과발현과 LRP6 가 저해된 심근세포에서는 이러한 apoptosis 신호 관련 단백질들의 발현을 증가시켰다. 이러한 결과는 LRP5 와 LRP6 는 저산소에 의해 발생하는 심근세포의 apoptosis 를 조절함으로서 심근세포의 보호 효과를 유도한다는 사실을 보여준다. 유전자 발현

분석 (mRNA-seq) 및 qPCR 결과는 LRP5 가 저산소 유도된 심근 세포에서 과발현 될 때, HIF-1α 표적 유전자의 전사 활성이 강하게 감소되는 반면, LRP5 의 침묵에 의해 현저하게 상향 조절됨을 확인하였다. 또한, LRP5 의 과발현은 저산소 조건 하에서 유비퀴틴-프로테아좀 경로를 통한 HIF-1α의 안정성을 악화시켰다. HIF-1α의 안정성 조절은 LRP5 가 PHD2 와의 결합에 의해서 HIF-1α의 산소-의존 분해 도메인 564 번 프롤린 잔기를 수산화시킴으로 발생하는 것을 확인하였다. 흥미롭게도, LRP6 는 PHD2 와 결합하지 않는 것으로 나타났다. 본 연구는 또한, LRP5 의 인산화가 HIF-1α 분해에 관여하고 Wnt/β-catenin 신호 전달 경로와 무관하다는 것을 확인 하였다. 위의 결과를 바탕으로, *in vivo* 에서 LRP5 조절에 의한 허혈 심근 손상정도를 확인하였을 때, LRP5 의 과발현은 높은 end-diastolic pressure-volume relationship (EDPVR) slope 와 심장기능을 평가하는 ejection fraction (EF), blood pressure 그리고 -dp/dt max 가 lacZ 대조군과 비교하여 감소되는 것을 확인하였다. 반대로, LRP5 가 저해된 심근경색 모델에서는, lamin 대조군과 비교하였을 때, 심근 손상이 예방되는 것을 확인하였다. 또한, TTC stanining 과 Masson's trichrome staning 을 통해, LRP5 조절 심근경색 동물모델에서 경색의 크기 및 섬유화 진행 정도를 확인하였을 때, LRP5 가 저해되었을 때 보다 작은 경색 크기와 섬유화를 관찰하였다. 이러한 결과를 통해, 본 연구에서는 심근경색에서 HIF-1α의 안정성을 조절할 수 있는 새로운 조절자로서 LRP5 의 역할을 규명하였고, 이는 LRP5 가 허혈성

심장질환을 제어할 수 있는 신규 표적이 될 수 있는 이론적인 근제를 제시 할 수 있는 것으로 생각된다.

1. Introduction

1.1. Myocardial infarction

Oxygen is an essential component of energy production and maintenance of life. The state of oxygen deficiency in tissues or organs, ‘ischemia’ or ‘hypoxia’, is more likely to occur locally than in whole body, it is a common feature associated with the cardiovascular disease like coronary artery disease (CAD) and myocardial infarction (MI) [1, 2]. Myocardial infarction occurs when blood flow decreases or stops to a part of the heart, leading to irreversible damage of myocardial tissue and permanent functional deficits [3]. The most common cause of a MI is the rupture of an atherosclerotic plaque on an artery supplying heart muscle [4]. Plaques can become unstable, rupture, and additionally promote the formation of a blood clot that blocks the left coronary artery; this can occur in minutes [5].

When an artery is blocked, heart triggers a process called the ischemic cascade; cardiomyocytes in the territory of the blocked coronary artery die (infarction), mainly through apoptosis and necrosis, and do not grow back. Cardiac fibroblast fills the spot and progresses fibrosis [6]. Since cardiomyocytes undergo terminal differentiation after birth, resulting in poor proliferation and regeneration after cell damage. Thus, cardiomyocyte death is important event underlying the development of cardiac dysfunction during pathological stress and determining the progression of cardiac abnormalities overtime.

MI is a global disease challenge that affects more than 40 million people worldwide [7]. Despite strides forward in the improvements and treatment of MI, heart failure which is a common complication of MI remains common, and the

incidence may be increasing owing to improved early survival with primary percutaneous coronary intervention [3]. Numerous studies have shown that a multiple factors influence development and progression of cardiac remodeling and LV dysfunction after MI. Although some drugs reduce mortality, current therapies to prevent or delay progression of MI are still limited. Therefore, understanding the molecular mechanisms of MI is crucial for identifying possible therapeutic targets and designing effective treatments.

1.2. Low-density lipoprotein receptor-related protein 5 (LRP5)

1.2.1. Structure of LRP5

LRP5 is a single-pass transmembrane receptor protein of the LDLR family [8, 9]. LRP5 has 1615 amino acids [Pubmed; AB017498.1], consisting of a large extracellular domain (ECD) of 1,400 amino acids and intracellular domain (ICD) of 215 amino acids (Figure 1). The ECD consists of four YWTD-type-propeller motifs, four epidermal growth factor (EGF)-like domains, and three LDLR type A (LA) domains [9]. The ECD mediates the interaction between LRP5 and extracellular ligands such as Wnt proteins, SOST, and Dickkopf (DKK-1) [10, 11]. Different ligands engage different YWTD/EGF-like domains to bind LRP5 [10]. Proper folding of the YWTD domain is necessary for LRP5 maturation and membrane localization, which is facilitated by the molecular chaperone Mesoderm development (Mesd) in mice [12]. The ICD of LRP5 consists of five PPP[S/T]P motifs and each juxtaposed with casein kinase 1 (CK1) sites [8], which is responsible for the signaling transduction. Both serine and threonine residues are phosphorylated by glycogen synthase kinase-3 (GSK-3), protein

kinase A (PKA) and CK1, and this dual phosphorylation is important for the recruitment of axin and GSK-3 upon Wnt binding to the receptor complex [13, 14].

As shown in Figure 1, LRP5 shares approximately 71% homology with LRP6 at the nucleotide level. These proteins have common domains structurally, including YWTD/EGF-like domains, LA domains, transmembrane and cytoplasmic domain [14]. Although LRP5 and LRP6 are typically described to act a similar role in that both are co-receptor for Wnt signal transduction, recent studies highlighted that LRP5 and LRP6 play distinct roles in tissue distribution and pathophysiological conditions [8, 9].

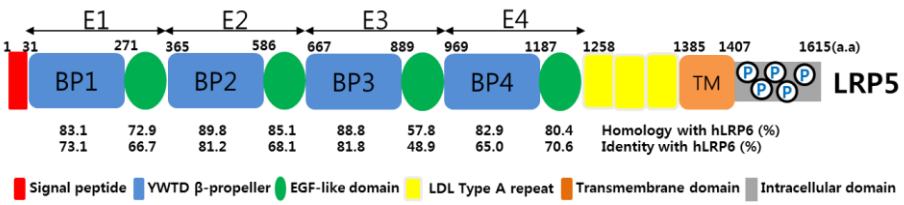

Figure 1. Domain structure of LRP5 and LRP6 [15].

1.2.2. Function of LRP5

LRP5 functions as an essential co-receptor for Wnt/β-catenin signaling activation which participates in embryonic development and physiological homeostasis in organisms [16, 17]. LRP5 is a widely expressed receptor in adult and embryonic tissues, including heart, liver, macrophages and bone, with the highest level of expression in the liver [18].

LRP5 do not have a NPxY motif which induces endocytosis separately from the other LDLR family, it has a distinct five PPP[S/T]P motifs in the intracellular domain (ICD). When PPP[S/T]P motifs of LRP5 is phosphorylated by Wnt ligands, LRP5 inhibits glycogen synthase kinase-3β (GSK-3β) phosphorylation by recruiting axin, scaffolding protein, then, β-catenin is stabilized in cytoplasmic and translocate into the nucleus. Nuclear β-catenin binds to TCF/LEF of transcriptional factors and activates transcription of downstream target genes (Figure 2) [8, 19-21].

The transcription of LRP5 gene is regulated by transcription factor KLF15, Sp1, FOXI1, FOXO4, HSF2, IRF-7A, RP58 and TBP. In addition, four other RUNX2 binding sites were identified in the 5' region of LRP5 as a regulator of LRP5 expression [22]. Post-translational modification by phosphorylation of the PPP[S/T]P motifs promotes an inducible docking site for axin [8].

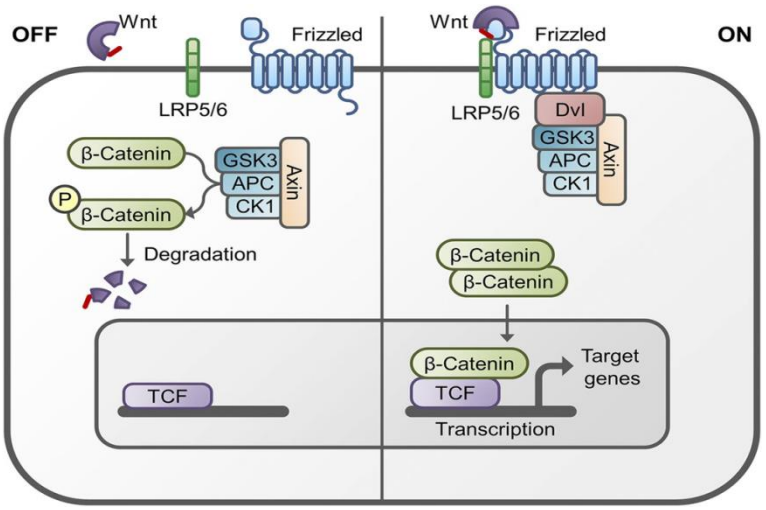

Figure 2. Overview of Wnt/ β-catenin signaling pathway [23].

1.2.3. LRP5 in human diseases

A loss-of-function mutations, gain-of-function mutation or altered expression of LRP5 have been implicated in a number of human diseases including osteoporosis [24], tumorigenesis [25, 26] and hypercholesterolemia [27].

Bone density disorders

LRP5 is well known to play a crucial role in bone mass density and development through Wnt/β-catenin signaling [16]. Loss-of function mutations in human LRP5 gene associated with osteoporosis pseudoglioma syndrome (OPPG), and gain-of function mutation cause the high bone mass (HBM) [28, 29]. Conditional deletion of LRP5 in mice showed low-bone mass phenotype evidence by demonstrating the decreased proliferation of osteoblast and bone formation [30]. In further studies for the role of LRP5 in bone mass, it was investigated that LRP5 G171V mutation in osteoblasts exhibits reduced osteoblasts and ostecytes apoptosis, increased osteoblastic activity, and causes high bone density [16, 31]. This LRP5 G171 site is located at the fourth blade of the first YWTD-type β-propeller, and its mutation into 171V was found to have the same activity of signal transduction for Wnt-1 ligand as normal LRP5. However, endogenous antagonist of Wnt signaling, Dickkopf-1 (DKK-1), was defective in this point mutation and this affected in increased Wnt/β-catenin signaling activity and promotes high bone mass [16]. Subsequent work has identified numerous additional mutations in LRP5 associated with alterations in human bone mass [29].

Moreover, LRP5 controls bone formation by inhibiting expression of TPH1, the rate-limiting biosynthetic enzyme for serotonin, a molecule that regulates bone formation, in enterochromaffin cells of the duodenum and that excess plasma serotonin leads to inhibition in bone [32].

Cancer

In relation to cancer initation and progression, LRP5 has been shown to be involved in breast cancer, skeletal metastasis prostate cancer (PCa) and osteosarcoma (OS) [25, 33, 34]. Tumorigenicity effect of LRP5 is mediated by Wnt/β-catenin signaling.

In breast human cancers, abnormally spliced internally truncated LRP5 (deletion of 142 a.a; LRP5Δ666–809) is frequently expressed in different cancer stage, including carcinoma *in situ* and metastatic carcinoma, which is resulted in increased accumulation of non-phosphorylated active β-catenin and transcription activity of β-catenin [25]. This LRP5Δ overlaps a binding site for the LRP5 antagonist DKK-1 ligand, and consequently DKK-1 could not inhibit transcriptional activity in breast tumors [25]. Moreover, in this study showed that breast tumor cell growth and metastasis are dependent on LRP5Δ in a xenograft SCID mouse model [25].

Osteosarcoma (OS) is the most common primary malignant tumor of bone, and expression profiling revealed that presence of LRP5 is significantly associated with tumor metastasis such as chondroblastic subtype of OS [34]. In this study, patients whose tumors were positive for LRP5 showed a trend toward to decreased event-free survival, suggesting that LRP5 is a novel marker for high-grade osteosarcoma progression [34].

In prostate cancer, the dominant-negative LRP5, which is inactivation of LRP5, resulted in mesenchymal to epithelial transition, blocking of translocation of β-catenin, increased PC-3 cell proliferation, suppressed migration and invasion *in vitro* [33]. In addition, in other cancers, LRP5 is required for maintaining the basal lineage of mouse mammary tissue [35] and for mammary ductal stem cell activity and Wnt1-induced tumorigenesis [36].

Coronary artery disease

Coronary artery disease is commonly resulted from abnormal cholesterol and glucose metabolism. Several studies have shown LRP5 may be involved in lipid metabolism. LRP5 binds apolipoprotein E (ApoE), and LRP5 expression is upregulated in the liver of $LDLR^{-/-}$ mice [37] and $ApoE^{-/-}$ mice fed with western diet [38]. Indeed, $LRP5^{-/-}$:$ApoE^{-/-}$ hypercholesterolemia mouse models have shown that LRP5 is necessary for calcification in the aortic valve [39]. The $LRP5^{-/-}$ mice fed a hypercholesterolemic diet have shown that developed aortic lipid infiltration and larger aortic atherosclerotic lesions by activating Wnt signaling [27, 40].

In separate study also showed that LRP5 deficient mice exhibit markedly impaired glucose tolerance and increased plasma cholesterol levels thought decreased hepatic clearance of chylomicron remnants. $LRP5^{-/-}$ mice had a marked reduction in the levels of intracellular ATP and Ca^{2+} in response to glucose; thereby, glucose-induced insulin secretion [41]. The role of LRP5 in cholesterol metabolism seems to be similar to other LDLR family functions such as LRP1 and LRP4, and is probably Wnt signaling in dependent [42].

1.3. Hypoxia inducible factor-1α (HIF-1α)

All organisms have an adaptive mechanism to maintain homeostasis for hypoxia, and which is mainly mediated by transcription factor, hypoxia inducible factor-1 (HIF-1) [43]. HIF-1 consists of an oxygen-responsive HIF-1α subunit and a constitutively expressed HIF-1β subunit (also kwnon as the aryl hydrocarbon receptor nuclear translocator; ARNT). Among them, HIF-1α is known as a main contributor in response to general acute cellular hypoxia. HIF-1α is ubiquitously expressed in different tissues and organs, whereas HIF-1β is constituvely expressed and its activity is regulated in an oxygen-independent manner [44]. Both are belongs to the bHLH-PAS family and share their protein domain structure, which is contains a bHLH (basic helix-loop-helix) DNA binding domain and a tandem of two PAS domains (PAS-A and PAS-B) for heterodimer formation between the HIF-1α and HIF-1β [45] [46]. Apart from these, HIF-1α contains an oxygen-dependent degradation (ODDD) involved in the regulation of protein stability, and two TAD domians (transactivation domains; TAD-N and TAD-C) for the regulation of protein function [46]. HIF-1 complex binds a core sequence of the HRE in the promoters of hypoxia-responsive genes and induces their expressions. More than 70 HIF-1α target genes have been identified including erythropoietin and GLUT1. These target genes increase oxygen availability, proliferation/survival factors and cellular glucose uptake [44, 47, 48].

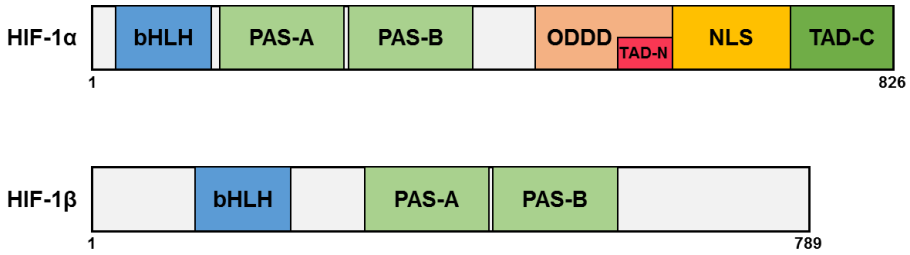

Figure 3. Domain structure of HIF-1α and HIF-1β [1]

1.4. Oxygen-dependent regulation of HIF-1α stability and activity

HIF-1α protein is tightly regulated by oxygen levels and its half-life is less than 5 minutes. However, hypoxia does not modify HIF-1α mRNA levels suggeting that the protein content of HIF-1α is regulated by its mRNA translation or by changes in tis rate of degradation [49].

Under nomoxic conditions, HIF-1α is rapidly degraded by hydroxylations of their proline residues in the HIF-1α degradation domian (ODDD domain) [6]. HIF-prolyl hydroxylases (PHD1–3) hydroxylates proline residues (Pro402 and Pro564 within the ODDD domain) of HIF-1α, and then induces interaction with the von Hippel–Lindau tumor suppressor protein (pVHL), which ultimately results in its proteasomal degradation [50]. VHL is the recognition component of E3-ubiquitin ligase that binds to HIF-1α for ubiquitinylation and rapid destruction by the 26S proteasome [51]. Under hypoxic conditions, however, HIF-1α is stabilized by limiting both hydroxylations by decreasing PHD activity. Stabilized HIF-1α is translocated into the nucleus and dimerized with HIF-1β. Then this complex binds to hypoxia-response elements (HREs), thereby up-regulates the

transcription of various genes involved in cell adaptation and survival under hypoxic conditions (Figure 4 and 5) [51, 52].

In parallel with this, a second oxygen-dependent repression of HIF-1α transcriptional activity is regulated by factor inhibiting HIF-1 (FIH-1). FIH-1 also regulates the ability of the HIF-1α in a hydroxylation-dependent switch. Under nomoxic conditions, FIH-1 hydroxylates asparagine-803 (Asn803) of HIF-1α within the C-terminal transactivation domain (TAD-C). Hydroxylated HIF-1α blocks the interaction with the transcriptional co-activator p300/CBP, thereby prevents transcriptional activation of the HIF-1 complex. Under hypoxic conditions, HIF-1α is activated by limiting hydroxylations by decreasing FIH activity (Figure 4).

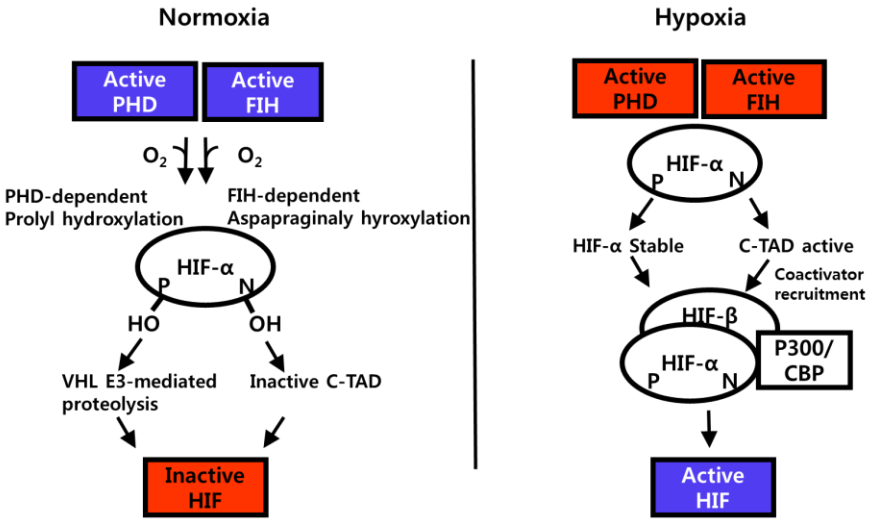

Figure 4. HIF-1α signaling pathway [1]

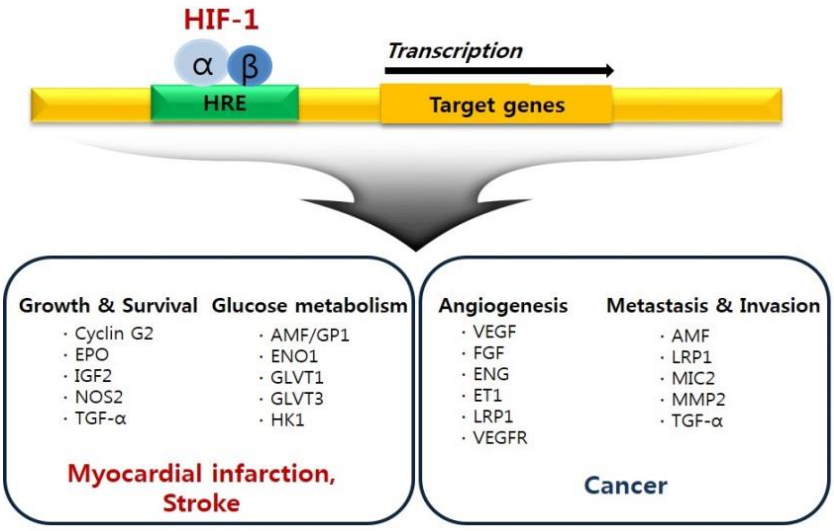

Figure 5. Target genes that are transcriptionally activated by HIF-1α [43].

1.5. Prolyl-4-hydroxylases (PHDs)

1.5.1. Characterization of PHDs

In mammals, three HIF-prolyl hydroxylase domain containing proteins (PHDs) PHD1 (also termed EGLN2, HPH3), PHD2 (EGLN1, HPH2) and PHD3 (EGLN3, HPH1) were identified to regulate the stability of HIF-1α [53]. Therefore, PHDs is known as a 'hypoxic senor' as its function is highly dependent on the amount of oxygen. PHD1-3 hydroxylate Pro564 of the ODDD of HIF-1a whereas Pro402 is only hydroxylated by PHD1 and PHD2.

PHDs belong to a family of the non-hem, iron (II) and 2-oxoglutarate-dependent dioxygenases. Members of the 2-oxoglutarate-dependent dioxygenases use oxygen, 2-oxoglutarate as co-substrates and iron (II) and ascorbate as cofactors for their enzymatic reaction. During catalysis, one oxygen atom is incorporated to a peptidyl proline of the substrate to form a hydroxyproline and the other oxygen atom is used for a coupled decarboxylation reaction that converts 2-oxoglutarate into succinate and CO_2 [44]. Both PHD1 and PHD2 have over 400 a.a residues (407 and 426 in human) and share a conserved prolyl hydroxylase catalytic domain at their c-terminal. PHD3 have much shorter a.a residues (239 a.a in human) than PHD1 and PHD2.

At the RNA level, PHD enzymes are widely expressed among different organs, although PHD1 strongly expressed in testis whereas PHD2 is highest in the heart [54]. PHDs are differentailly localized on the intracellular. PHD1 is exclusively localized in the nucleus whereas PHD2 was found in the cytosol. PHD3 was equally detected in both compartments [55] [56]. Endogenous PHD2

and PHD3 were described in the cytoplasm as well as in the nucleus. In hypoxia, PHD2 remained in the cytoplasm [57].

1.5.2. Regulation of PHD expression and activity

Proline hydroxylation is a non-reversible process and therefore PHDs itself are regulated on protein as well as on RNA levels. PHD2 and PHD3, but not PHD1 mRNA expression is oxygen-dependently regulated by HIF [58]. Enhanced hydroxylation activity due to increased PHD protein amount upon hypoxia accelerated HIF-1α protein degradation during reoxygenation process [59]. Moreover, in long-term hypoxia increased PHD2 and PHD3 protein levels can compensate for reduced pO_2 and attenuate HIF-1α protein levels and its target genes limiting the hypoxic response [60].

Activity of PHDs is usually regulated by oxygen. The changes in oxygen easily limit prolyl hydroxylation and indicate the PHDs are effective oxygen sensors. Moreover, PHDs activity also affects by energy metabolites, irons, nitric oxide and ROS. However, PHDs are might regulated their activity by interacting with other proteins.

1.5.3. PHD2

PHD2 has been proposed to be the main oxygen sensor. Downregulation of PHD2 by siRNA was sufficient to stabilize HIF-1α under normoxic condition. However, different PHD expression levels in different cell lines do contribute differently to the regulation of HIF- 1α protein [47]. PHD2 and PHD3 are expressed mainly in heart and skeletal muscle, particularly, PHD2 is known as main HIF-1α modulating in heart.

PHD2 consists of a catalytic domain that consists of a prolyl hydroxylase catalytic subunit and a MYND (myeloid, nervy and DEAF-1) zinc finger domain (Figure 5). MYND domain functions as a protein-protein interaction domain that provides the basis for negative transcriptional regulation. Deletion of the MYND-type zinc finger in PHD2 has been reported to enhance its activity and it is proposed that the PHD2 N-terminal region negatively modulates PHD2 catalytic activity [61].

In pathological conditions, downregulation of PHD2 by RNAi in mice attenuated ischemia/reperfusion injury of the heart and decreased infarct size [62]. Moreover, recent study reported that administration of the prolyl hydroxylase inhibitor, dimethyloxallyl glycine (DMOG), 24 hours before the onset of ischemia significantly reduced postischemic infarct size in rabbit hearts [63]. In tumors, enhanced PHD2 expression correlates with increased aggressiveness of tumors [48].

Figure 6. Domain structure of PHD2

1.5. Purpose of this study

LRP5 is clearly known as a Wnt co-receptor for transduce canonical Wnt/β-catenin signaling pathway. Although inhibition of Wnt/β-catenin signaling has been reported to protect myocardial death against ischemia/reperfusion (I/R) injury [64-67], neither the LRP5 involved nor the underlying mechanisms have been identified. Recent studies demonstrated that double deletion of LRP5 and LRP6, sister isoform to LRP5, promotes ischemia-induced DNA-damage in *in vivo* [68] and $LRP6^{+/-}$mice promotes larger stroke in brain ischemic injury [69]. Another recent study reported that $LRP5^{-/-}$ mice had worsen myocardial remodeling after acute MI via abrogated Wnt signaling pathway [70]. However, Genetic studies have shown that LRP5 is not optimized for stimulating β-catenin/TCF signaling [71] rather than LRP6 [72], which is suggesting that LRP5 structure and function may be optimized to perform a different function in Wnt-independent manner. Indeed, it was reported that LRP5 controls glucose uptake and growth of mammary epithelial cells, but not because of its role in Wnt signaling. In addition, LRP6 has little impact on this effect [73]. Moreover, deficiency of LRP6 in heart have been shown that disrupted gap junction formation by modulation of connexin 43 (Cx43), but LRP5 does not contribute to the regulation of Cx43 gap junction [74]; further supporting LRP5 might be having a unique role in pathophysiological conditions, especially, ischemic myocardium. Therefore, the aim of this study was to investigate the expression and function of LRP5 in ischemic myocardium.

In this study identified a novel molecular property of LRP5 in regulating PHD2-mediated HIF-1α stability in ischemic myocardium. Overexpression of LRP5 promotes proteosomal degradation of HIF-1α by interacting with PHD2

under hypoxic condition, which resulted in hypoxia-induced cardiomyocytes death. This study also found that the LRP5-mediated stability of HIF-1α is independent of Wnt/β-catenin signaling, which is mediated by phosphorylation of LRP5. In summary, this study reveals an important mechanism underlying the role of LRP5 in myocardium infarction.

2. Materials and Methods

2.1. Primary culture of rat cardiomyocytes

Neonatal rat cardiomyocytes were isolated from the hearts of 2-4day-old Sprague-Dawley rats. Briefly, isolated hearts were washed with Dulbecco's phosphate-buffered saline solution (pH 7.4, WELGENE) and minced to approximately 0.5 mm^3 sized pieces. The heart tissues were then treated with 5 mL collagenase II (1.4 mg/mL, 270 units/mg, Gibco BRL) solution for 5 min, the supernatant was removed and then washed with alpha modification minimum essential medium (α-MEM) with 10% fetal bovine serum (FBS) and 1 % penicillin/streptomycin solution (Carpricorn Scientific GmbH). The pellet was suspended with collagenase II and incubated in a 37℃ humidified atmosphere chamber containing 5% CO_2 for 7 min. This procedure was repeated until the tissue was completely digested. The resulting cell pellet was suspended with α-MEM and cells were attached in 100-mm culture dish for 30min at 37℃. Non-adherent cardiomyocytes were cultured for experiment with α-MEM containing 10% FBS, 1% penicillin/streptomycin solution and 0.1mM bromodeoxyuridine (BrdU, Sigma-Aldrich) to eliminate fibroblast expansion.

2.2. Construction of adenoviral vector

Recombinant adenoviruses that expressing full-length human LRP5 with a C-termial Myc tag (named as Ad-LRP5) and full-length human LRP6 with a C-termial VSVG tag (named as Ad-LRP6) were constructed using a ViraPower™ Adenovirus Expression System (Invitrogen). An adenoviral vector expressing lacZ-b-galactosidase (named as Ad-lacZ) was used as an infection control. The constructs were then used in a LR recombination reaction with the

pAd/CMV/V5/DEST gateway vector to generate an adenoviral expression clone. Then, the constructed adenoviral vector was transfected into 293A cells using lipofectamine 2000 reagent (Invitrogen life Technologies) after digesting with the Pac I restriction enzyme. Adenoviral particles were tittered using the Adeno-X™ qPCR titration kit (Takara, Clontech). Isolated cardiomyocytes were infected with Ad-LRP5 (multiplicities of infection (MOI) of 10) or Ad-LRP6 (MOI of 10) for 48h before exposed to hypoxic condition. The shRNA targeting rat LRP5 (named as shLRP5) and rat LRP6 (named as shLRP6) were generated using a BLOCK-iT™ Adenoviral RNAi Expression system (Invitrogen). The RNAi nucleotide sequence targeting rat LRP5 is 5′-GCUGUUCAGCCAGAAAUUU-3′ and rat LRP6 is 5′-GGUUGUUCCCAUUUGUGUU-3′. Double-stranded oligonucleotide s cloned in the BLOCK-iT™ U6 entry vector were used in a LR recombination reaction with pAd/BLOCK-iT™-DEST vector to generate an adenoviral expression clone. The pAd-GW/U6-lamin^{shRNA} adenoviral vector (named as lamin) was used as an infection control. Adenoviral particles were tittered using the Adeno-X™ qPCR titration kit (Takara, Clontech). Isolated cardiomyocytes were infected with shLRP5 (MOI of 40) or shLRP6 (MOI of 40) for 72h before exposed to hypoxic condition.

2.3. Hypoxia treatment

Cardiomyocytes were washed 2 times with hypoxic media (serum free and replacing with N_2 gas for 30min). Hypoxic condition was obtained by placing the cells into a modular incubator chamber (Vision Scientific, Republic of Korea), which was connected to a gas bottle containing a mixture of 5% H_2, 5% CO_2, and 95% of N_2. A continuous slow flow (0.1 L/min) was applied throughout the

experiment. To obtain normoxia, we used a gas mixture of 21% O_2, 5% CO_2, and 74% of N_2.

2.4. Cell viability

For cell viability assay, experimental cells were evaluated by both the MTT and trypan blue assay. MTT assay was measured by CellTiter 96 Aqueous One Solution Cell Proliferation Assay (Promega) according to the manufacturer's instructions. The absorbance was measured at 490 nm using an ELISA reader (TECAN, infinite M200 PRO). For Trypan blue assay, cells were detached by trypsinization and stained with 0.4% Trypan blue dye. The number of viable cells was counted under microscope using a hemacytometer counter. The viability of the control was regarded as 100%.

2.5. Luciferase reporter assay

Luciferase reporter construct containing three HREs was purchased from Addgene (26731). HRE-luciferase reporter plasmid and renilla luciferace vector (pRL-TK; Promega) were transiently transfected into control, LRP5-overexpressed- or LRP5-silenced cardiomyocytes for 24h. Next, cells were exposed to normoxic or hypoxic condition. Cell lysate was harvested for both *firefly* and *Renilla* luciferase assay analysis using the Dual-Luciferase Reporter Assay System (Promega), as described in the manufacturer's protocol. HRE-Luciferase activity was measured using a Micro-Lumat Plus LB96V luminometer (EG&G Berthold). Data were normalized to the *Renilla* luciferase activity to account for differences in transfection activity.

2.6. Nuclear extract preparation

Cells were lysed with cytosol extraction buffer (10mM HEPES; pH7.5, 3mM $MgCl_2$, 14mM KCl, 5% glycerol and 1mM DTT) for 10min on ice, then NP-40 at a 0.4% final concentration was added and vortexed for 10s. The cell suspensions were centrifuged for 2min at 5000rpm at 4℃, then supernatant containing the cytosolic fraction were removed. The pellet were washed in the same lysis buffer for 3 times, then lysed with nuclear extraction buffer (10mM HEPES; pH7.5, 3mM $MgCl_2$, 400mM NaCl, 5% glycerol and 1mM DTT) and sonicated. After 30min of incubation, the pellet suspensions were centrifuged for 10min at 14000rpm at 4℃. Supernatant containing the nuclear fraction were used for western blotting. Anti-lamin B and anti-α-tubulin were used as nuclear and cytoplasmic loading controls, respectively.

2.7. Apoptosis assay

Hypoxia-induced cardiomyocytes apoptosis rate was determined by using the Annexin V-Cy3 apoptosis detection kit (Sigma-Aldrich) or colorimetric Caspase 3 Assay kit, (Sigma-Aldrich) according to the manufacturer's instructions, respectively. Annexin V-Cy3 labeled cells were then visualized by a laser scanning confocal microscope (Fluoview FV1000, Olympus). For the detection of Caspase-3 activity, cell lysate was combined with an equal amount of substrate reaction buffer with a caspase-3 colorimetric substrate (Ac-DEVD-pNA), and then absorbance was measured at 405 nm using an ELISA reader (TECAN, infinite M200 PRO).

2.8. PHD2 activity assay

Biotinylated HIF-1α oxygen-dependent degradation domain (Biotin-DLDLEALAPYIPADDDFQL; from amino acids 556 to 575 of HIF-1α) and a hydroxylated control (Biotin-DLDLEALAP[OH]YIPADDDFQL) peptides were immobilized on streptavidin and BSA-coated 96 well plates. Cells were harvested and lysed with hypotonic buffer (20mM HEPES; pH7.4, 5mM NaF, 10μM Na_3VO_4, 0.1mM EDTA, protease inhibitor cocktail, and 2mM DTT) for 20min, then NP-40 at a 0.5% final concentration was added. Equal quantities of protein (50μg/well) were incubated with reaction buffer (Tris-Cl; pH7.5, 5mM KCl, 1.5mM $MgCl_2$, 2mM DTT, 0.5mM 2-OG and 1mM ascorbate) for 1h at RT. Sample were incubated with hydroxylated HIF-1α primary antibody, followed by addition of a goat anti-rabbit HRP-conjugated secondary antibody. Peptide hydroxylation was detected using a TMB substrate at 650nm.

2.9. Immunoprecipitation assay and western blotting

Cells were lysed in RIPA buffer containing protease inhibitor cocktail and 1mM phenylmethylsulfonyl fluoride (PMSF). Protein concentrations were determined using a Bradford Protein Assay Kit. Equal quantities of protein were separated by 6-12% SDS-PAGE and transferred to a polyvinylidene difluoride (PVDF, Bio-Rad) membrane. The membranes were incubated with primary antibodies using the following antibodies for overnight at 4℃: rabbit anti-HIF-1α (NB100-479), rabbit anti-PHD2 (NB100-2219), rabbit anti-PHD3 (NB100-139) from Novus Biologicals; rabbit anti-LRP5 (5731), rabbit anti-LRP6 (2560), rabbit anti-Hydroxy-HIF (Pro564) (3434P), rabbit anti-Bax (2772), mouse anti-Myc tag (2276) and rabbit-anti LRP6 (phospho S1490) (2568) from Cell Signaling Technology; rabbit anti-β-catenin (ab32572), rabbit anti-PHD1 (ab113077) and

rabbit anti-LRP5 (phospho T1492) (ab203306) from Abcam; Mouse anti-Bcl-2 (610538) from BD Biosciences; rabbit anti-VSVG tag (ADI-MSA-115) from Enzo Life Sciences. The blots were washed 5 times for 25min with TBS-t (0.1% Tween 20) and then incubated with a horseradish peroxidase-conjugated secondary antibody for 1h at RT. Immuno-reactive proteins were detected using an ECL system (iNtRON Biotechnology). ImageJ software was used for quantification. For the immunoprecipitation assay, lysates were precleared with protein A/G-Agarose beads (Santa Cruz Biotechnology) prior to adding the antibody. Then, after removing the protein beads by centrifugation, the supernatant was incubated overnight at 4℃ with the primary antibodies against mouse anti-myc tag (2276) from Cell Signaling Technology, mouse anti-PHD2 (AM09354PU) antibodies from Origene Technologies or isotype control immunoglobulin G (sc-2025) from Santa Cruz Biotechnology. Next, A/G-Agarose beads were added, and incubated for 4h at 4℃ with rotation, and then bead-antibody complexes were washed 4 times with EBC washing buffer (20mM Tris, 500mM NaCl, 1mM EDTA, 0.5% NP-40). Immunoprecipitated proteins were denatured in SDS sample buffer and boiled for 5min. Samples were analyzed by western blotting.

2.10. Gene expression analysis

Total RNA from lacZ-Ad infected-normoxic control and hypoxia-induced lacZ-Ad, LRP5-Ad or shLRP5-infected cells was isolated using a Trizol reagent (Invitrogen, USA). The mRNA sequencing and analysis were performed by e-biogen Company. A p-value of < 0.05 was used to generate lists of differentially

expressed genes. Gene Ontology enrichment analysis and KEGG enrichment analysis was conducted using the DAVID tool (http://david.abcc.ncifcrf.gov/).

2.11. Quantitative real-time PCR (qPCR) analysis

Total RNA was isolated from cells using a Trizol reagent (Invitrogen, USA) and was reverse transcribed to cDNA with a 1st Strand cDNA Synthesis kit (Takara, Japan). For qPCR analysis, the Roter-Gene 3000 (Corbett Research, Australia) was used with the RealHelix^{TM} SYBR premix qPCR kit (NanoHelix, Republic of Korea). Gene expression was normalized to GAPDH. The relative mRNA expression levels were quantified and analyzed using Rotor-Gene 6 software (Corbett-research, Australia) using $^{\Delta\Delta}$Ct methods. PCR primers used in this study are listed in Table 1.

Table 1. The sequences of primers used for qPCR analysis.

Genes	Primer (5'-3')
LRP5	Forward: AGGCCCTACATCATTCGAGG Reverse: GGGGTCTGAGTCCGAATTCA
PFKFB3	Forward: CAGTCCTGAAACTGACGC Reverse: GACAGCCTCTGACCTCTC
NOS2	Forward: CTCACTGTGGCTGTGGTCACCTA Reverse: GGGTCTTCGGGCTTCAGGTTA
GLUT-1	Forward: GCCTGAGACCAGTTGAAAGCAC Reverse: CTGCTTAGGTAAAGTTACAGGAG
Bnip3l	Forward: CTGCACTTCAGCAATGGG Reverse: CTCTTGGAGCTGCTTCGT
EPO	Forward: AGGGTCACGAAGCCATGAAG Reverse: GATTTCGGCTGTTGCCAGTG
VEGF	Forward: TTACTGCTGTAC CTCCACC Reverse: ACAGGACGGCTTGAAGATG
HIF-1α	Forward: GGTGGATATGTCTGGGTTGAG Reverse: TTCAACTGGTTTGAGGACAGA

PHD1	Forward: GCT GCTGCGTTGGTTAC Reverse: GCCTCCTGGTTCTCTTG
PHD2	Forward: CTGGGACGCCAAGGGA Reverse: CAATGTCAGCAAACTGG
PHD3	Forward: GTTCAGCCCTCCTATGC Reverse: ACCACCGTCAGTCTTTA
β-catenin	Forward: AGGGGTCCTCTGTGAACTTG Reverse: CAGCAGTCTCATTCCAAGCC
Wnt3a	Forward: ATTTGGAGGAATGGTCTCTCG Reverse: GCAGGTCTTCACTTCGCAAC
Axin2	Forward: CGCTAGGCGGAATGAAGA Reverse: GTATGCACCATCTTGGTC
GAPDH	Forward: CAGTGCCAGCCTCGTCTCAT Reverse: TGGTAACCAGGCGTCCGATG

2.12. Immunofluorescence staining

Cardiomyocytes were plated in 24-well cell culture slides (BD Biosciences) with cover glass and cultured at 37℃ for 24 h. After 24 hours, cells were infected with Ad-lacZ, Ad-LRP5 or shLRP5 for 48h, cells were then exposed to hypoxia for 2 hours. Cells were immobilized with 4% paraformaldehyde for 10 min followed by incubation with 0.2% Triton X-100 for 10 min at room temperature. After permeabilization, cells were washed 3 times with PBS then blocked with 2% bovine serum albumin (BSA) in PBS 1 hours. Cells were incubated with rabbit anti-HIF-1α (NB100-479) as primary antibody overnight at 4℃, and then stained with mouse anti-rabbit IgG-TR (Santa Cruz Biotechnology) at RT for 1h in dark. The cell's nucleus was stained with 0.2μg/ml DAPI (Sigma-Aldrich) for 1min. Finally, the cells were visualized by laser scanning confocal microscope (Fluoview FV1000, Olympus).

2.13. X-Gal staining of tissues

For visualization of β-galactosidase activity, lacZ adenovirus-injected fresh rat heart tissues were excised and post-fixed with 4% paraformaldehyde for 4h at 4℃, and then incubated with 30% sucrose overnight at 4℃. The heart tissues were mounted on standard cryomold with OCT compound, and cut into 20 μm serial-sections using a cryostat (Thermo Fisher Scientific). Then, serial sections were stained overnight at 37℃ with X-gal using the senescence β-galactosidase histochemical staining kit (Sigma-Aldrich). Stained sections were captured by microscope (Olympus, USA).

2.14. Histological analysis and immunohistochemistry

For histological analysis and immunohistochemistry, the hearts were excised and fixed with 4% formaldehyde. After dehydration, the heart tissues were embedded in paraffin wax and sectioned at 4-μm thickness. The levels of collagen deposition were determined by Masson's trichrome staining (American MasterTech, USA). Areas of fibrosis tissue and total tissue in each field were measured and evaluated as a percentage of fibrosis tissue area to total tissue area using a SABIA (Solution for Automatic Bio-Image Analysis) program (e-Biogen, republic of Korea). In addition, immunohistochemistry was performed according to the avidin biotinylated-horse radish peroxidase (HRP) complex (ABC)-based method using a Vectastain ABC kit (Vector Laboratories). Briefly, paraffin-embedded heart sections were deparaffinized and rehydrated through xylenes and graded ethanol series prior to antigen retrieval. The sections were then incubated with 0.3% hydrogen peroxide in 60% methanol for 30 min and blocked with normal goat serum for 1h at 4℃. This was followed by incubation with the primary antibodies. Immunoreactivity was achieved using a 3-3′-

diaminobenzidine (DAB, Sigma-Aldrich). The sections were counterstained with Mayer's hematoxylin solution (Sigma-Aldrich,), dehydrated, defatted, and mounted with malinol (Muto Pure Chemicals). The stained structure was observed under a microscope (BX41, Olympus). The Image J software was used for quantification. Five images of non-overlapping fields of stained sections were captured from each section per animal by microscope (Olympus, USA), and quantitative analysis of positive staining areas (%) in images was done by using Image J software (NIH, USA).

2.15. Animals

Spraque Dawley Rat (7weeks old) and neonatal rat on Spraque Dawley background were purchased from Samtako Bio Korea company under specific pathogen-free (SPF) conditions. Animals were fed a standard laboratory diet with water and kept on a 12h light/12h dark cycle in a temperature-controlled room. All animal studies were conducted in accordance with the International Guide for the Care and Use of Laboratory Animals. The protocol was approved by the Animal Research Committee of the Chosun University School of Medicine (Protocol No. CIACUC2018-S0004).

2.16. Animal model of ischemia/reperfusion injury

Ischemic/reperfusion (I/R) model was established in 7-week-old Sprague-Dawley male rats (250g) by surgical occlusion of the left anterior descending (LAD) coronary artery as described previously.[75, 76] Briefly, rats were anesthetized and ventilated with room air via tracheal intubations connected to a Harvard ventilator. Following left lateral thoracotomy located between the third

and fourth ribs, the pericardium was incised and the left anterior descending coronary artery was ligated by a sterile 6-0 silk suture. Proper ligation for myocardial infarction model was verified by visual observation of the left ventricle wall turning pale. After 60 minutes of regional myocardial ischemia, the ligation was released after removal of the 6-0 silk suture to allow reperfusion. Sham-operated animals underwent same procedure without occlusion of the LAD coronary artery. To determine the effect of LRP5 in myocardial infarction models in vivo, animals were injected with adenoviral constructs either expressing lacZ, LRP5, lamin or shLRP5 (2×10^{11} particles) before performing the operation. The adenovirus constructs were injected at three injection sites into the anterior left ventricular free wall using a 32G needle. Sham-animals were injected with saline. Adenovirus infection efficiency was assessed using western blot analysis after 3 days. Sham, Ad-lacZ, Ad-LRP5, lamin, shLRP5 injected experimental animals were re-anesthetized 3 days later and performed left anterior descending coronary artery ligation.

2.17. Infarct size determination

Sham and ischemic/reperfusion (I/R)-injured animals were euthanized at 2weeks after operation and their hearts were excised and washed with PBS. The heart was snap frozen in liquid nitrogen and sectioned transversely, and incubated in 1% 2,3,5-Triphenyltetrazolium chloride (TTC) solution (pH 7.4 buffer at 37℃) for 20 minutes. The tissue was immersed in 10% PBS buffered formalin overnight at 4℃. The size of myocardial infarction was evaluated as a percentage of the sectional area of the infarcted tissue of the left ventricle to the sectional

area of total ventricular area. Planimetry was used to assess overall infarct size using Image J software (NIH, USA).

2.18. Hemodynamic analysis

Hemodynamic assessment was performed using a Mikro-Tip Research Pressure System (Millar Instruments). Briefly, rats were anesthetized and 2F Pressure-volume (P-V) catheter (SPR-838, Millar Instruments) was inserted into the right carotid artery and advanced into the ascending aorta. Then, the catheter was advanced into the LV cavity until stable P-V loop were obtained. EF, Heart rate, dP/dt max and dP/dt min were computed and calculated using a PV analysis program (PVAN, Millar Instruments). The slope (Ees) of the LV end-systolic P-V relationship (ESPVR) was calculated as load-independent indices of LV contractility. At the end of each experiment, 100μl of hypertonic saline was injected intravenously, and from the shift of P-V relations, parallel conductance volume was calculated by the software and used for the correction of the cardiac mass volume. Finally, the data were analyzed using the LabChart data analysis software.

2.19. Statistical analysis

All quantified data from at least triplicate samples were analyzed with SPSS 13.0 software. Data are expressed as mean ± SD. Statistical comparisons between two groups were performed using Student's t-test. Statistical comparisons among multiple groups were performed using analysis of variance (ANOVA). A two-tailed $P < 0.05$ was considered statistically significant.

3. Results

3.1. Expression of LRP5 and LRP6 in hypoxia-induced cardio-myocytes

Although LRP5 and LRP6 are structurally similar and serve as a co-receptor for Wnt signal transduction, they display clearly distinct function according to tissue distribution and pathophysiological conditions [19, 41, 73, 74]. To understand the molecular basis that account for the different role of LRP5 and LRP6 in ischemic myocardium, this study first identified the expression level of LRP5 and LRP6 in hypoxia-induced cardiomyocytes.

As shown in Figure 7A, the expression of LRP5 was significantly upregulated in hypoxia-induced cardiomyocytes compared to normoxic cells, whereas LRP6 expression was downregulated under hypoxic condition. Moreover, qPCR and western blot analysis demonstrated that hypoxia induced LRP5 mRNA and protein expression in a time-dependent manner (Figure 7B).

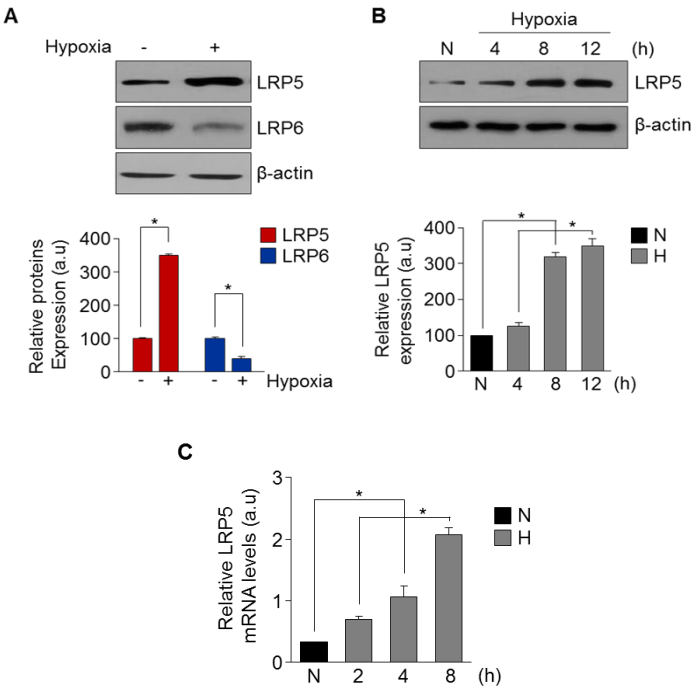

Figure 7. Effect of hypoxia on LRP5 and LRP6 expression in cardiomyocytes

Cardiomyocytes were exposed to normoxia (indicated by "N") or hypoxia (indicated by "H") (O_2 1.2%) at the indicated times and harvested for western blotting and RNA extraction. (A) Cardiomyocytes were exposed to hypoxia for 8h. The expression of LRP5 and LRP6 were analyzed by western blotting (n=4). Protein levels were normalized to β-actin levels. (B) The expression levels of LRP5 were analyzed by western blotting (n=3). Protein levels were normalized to β-actin levels. (C) The mRNA levels of LRP5 were quantified by qPCR (n=4). Gene expression was normalized to GAPDH. Values are represented as mean ± SD. *P < 0.05 compared with normoxia.

3.2. Adenovirus expressing LRP5/6 or shLRP5/6

To investigate the effects of LRP5 and LRP6 in hypoxia-induced cardiomyocytes, this study used adenoviral vectors to overexpress the myc tagged-LRP5 (Ad-LRP5) and VSVG tagged-LRP6 (Ad-LRP6) cDNA or to express an LRP5 and LRP6 targeting shRNA (shLRP5 or shLRP6) for silencing endogenous expression. LacZ-β-galactosidase (Ad-lacZ) and lamin were used as an infection control against Ad-LRP5/6 or shLRP5/6, respectively.

To assess the adenoviral transduction efficiency, cardiomyocytes were infected with LRP5/6 or shLRP5/6 at different MOIs and times. As shown in Figure 8A-D, LRP5/6 and shLRP5/6 adenoviral vectors were successfully constructed for infection into cardiomyocytes. In this study, Ad-LRP5 and Ad-LRP6 infected cells with MOI of 10 for 48h, and shLRP5 and shLRP6 infected cells with MOI of 40 for 72h.

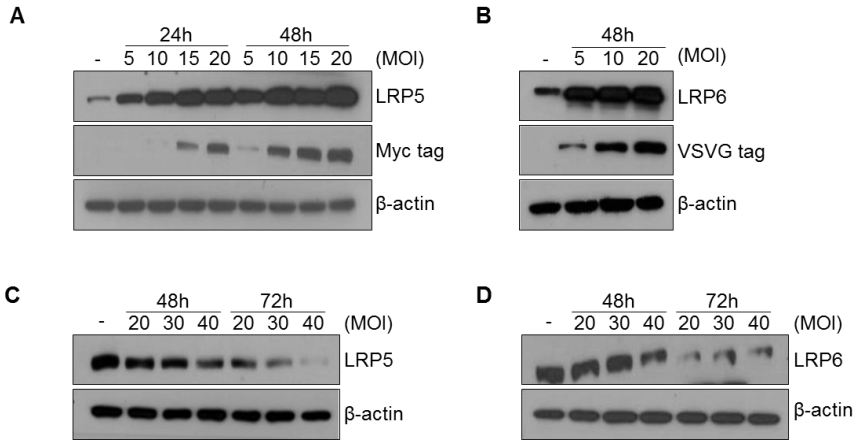

Figure 8. Construction of LRP5/6 or shLRP5/6 adenoviral vector

Cardiomyocytes were infected with adenoviruses expressing full-length LRP5/6 or shRNA targeting LRP5/6 at the indicated MOI values and times. Adenoviral transduction efficiency was assessed by western blotting. (A) Representative western blot images of cells infected with Ad-LRP5 (Myc tagging) (n=3). (B) Representative western blot images of cells infected with Ad-LRP6 (VSVG tagging) (n=3). (C) Representative western blot images of cells infected with shLRP5 (n=3). (D) Representative western blot images of cells infected with shLRP6 (n=3).

3.3. Effect of LRP5 and LRP6 on cell viability under hypoxic condition

To investigate the effects of LRP5 and LRP6 on cell survival of cardiomyocytes under hypoxic condition, MTT assay and trypan blue staining were performed. As shown in Figure 9A-D, hypoxia decreased the cell viability by approximately 50% in Ad-lacZ and lamin control cells. Overexpression of LRP5 led to further decrease of cell viability by approximately 23% (for trypan blue assay) and 12% (for MTT assay) compared to Ad-lacZ control cells (Figure 9A and B), whereas overexpression of LRP6 had no significant difference on cell viability compared with Ad-lacZ control cells (Figure 9A and B). Moreover, the survival rates of the cardiomyocytes were highly increased in the LRP5-silenced cells (Figure 9C and D). However, silencing of LRP6 further decreased cell viability by approximately 28% (for trypan blue assay) and 14% (for MTT assay) (Figure 9C and D). These finding suggested that silencing of LRP5 prevents cardiomyocytes death against hypoxic condition, also indicated the possibility that LRP5 and LRP6 may display converse function in hypoxia-induced cardiomyocytes death.

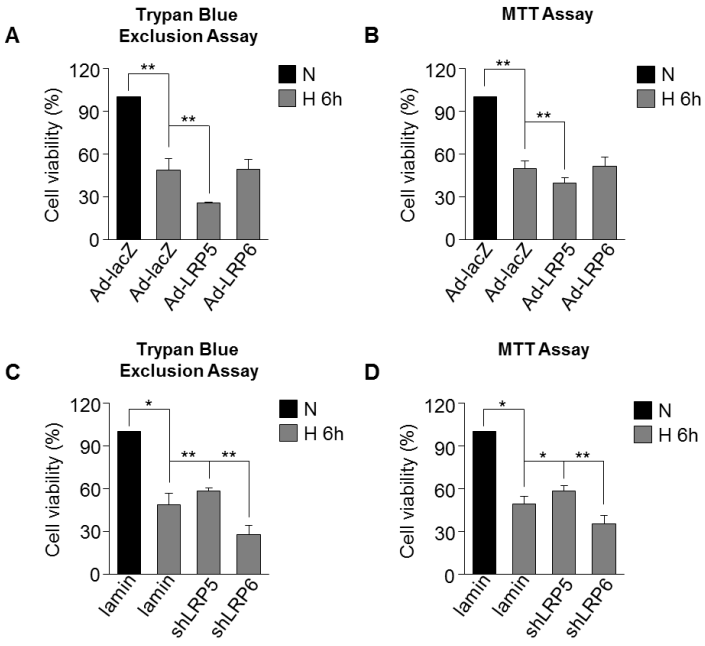

Figure 9. Effect of LRP5 and LRP6 on cell viability in hypoxia

Cardiomyocytes were exposed to normoxia or hypoxia for 6h and analyzed for cell viability using a trypan blue exclusion assay and MTT assay. Evaluation of cardiomyocytes cell viability by (A) trypan blue exclusion and (B) MTT assay in LRP5 or LRP6 overexpressed-hypoxic cells. Cell viability was normalized with normoxic Ad-lacZ control cells (n=4). Evaluation of cardiomyocytes cell viability by (C) trypan blue exclusion and (D) MTT assay in LRP5 or LRP6 silenced-hypoxic cells. Cell viability was normalized with normoxic lamin control cells (n=4). Values are represented as mean ± SD. *P < 0.05 and *P < 0.01 compared with normoxia.

3.4. Effect of LRP5 and LRP6 on the apoptosis signal pathway

Myocardial apoptosis is a contributing factor to ischemia/reperfusion (I/R) injury and the loss of viable myocardium [77]. To further investigate that the cellular death mechanism is due to apoptosis signal pathway, apoptotic molecules, such as caspase-3 activity, Annexin-V and Bax/Bcl-2 expression were assessed. Early apoptotic cells were measured by detection of Annexin V-Cy3.18 using a confocal microscope. Cardiomyocytes were exposed to acute hypoxia (O_2 1.2%) for 2h, and representative fluorescence image of Annexin V are shown in Figure 10A and B. Overexpression of LRP5 caused a significant increase of Annexin-V detection ratio compared to Ad-lacZ control cells under hypoxic conditions. Moreover, silencing of LRP5 significantly inhibited apoptotic cells compared with hypoxic lamin control cells. As shown in Figure 10C and D, late-apoptotic maker, caspase-3 activity was increased in LRP5-overexperssed cells compared with Ad-lacZ control cells, whereas silencing of LRP5 attenuated caspase-3 activity under hypoxic condition. Unlike the MTT and trypan blue assay results in Figure 9A and B, overexpression of LRP6 decreased caspase-3 activity, whereas silencing of LRP6 further increased caspase-3 activity compared to hypoxic lamin control cells (Figure 10C and D).

To assess whether LRP5 and LRP6 regulates pro-apoptotic gene such as BaX and anti-apoptotic gene such as Bcl-2, expression analysis was performed. As shown in Figure 11A and D, significant higher in Bax/Bcl-2 ratio was detected in Ad-LRP5 or shLRP6-infected cardiomyocytes compared to each control cells. In contrast, Ad-LRP6 or shLRP5-infected cells decreased Bax/Bcl-2 ratio (Figure 11B and C). These findings suggest that silencing of LRP5 increases cell survival and inhibits apoptosis by regulating the apoptosis down-stream signal pathway,

Bax, Bcl-2 and cleaved caspase-3. Taken together, these finding demonstrating that LRP5 and LRP6 have a distinct role under acute hypoxic condition.

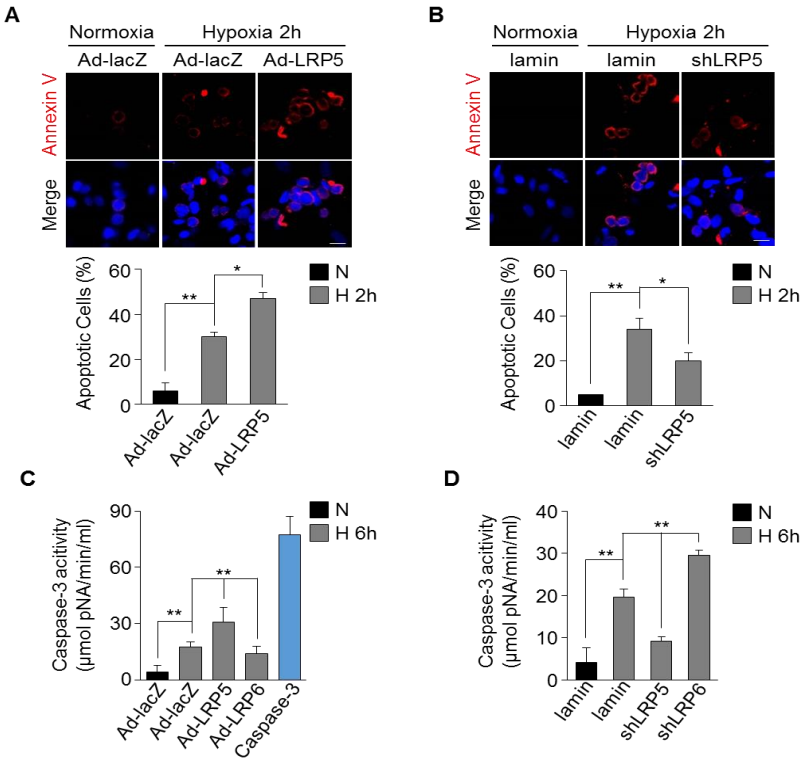

Figure 10. Effect of LRP5 and LRP6 on apoptotic markers under hypoxic conditions

Cardiomyocytes were infected with Ad-lacZ, Ad-LRP5/6, lamin or shLRP5/6, respectively, then exposed to normoxia or hypoxia (O_2 1.2%) for the indicated times. (A)(B) Representative fluorescence image of cardiomyocytes apoptosis stained with Annexin V-Cy3.18 (red) (n=4). Nuclei were stained with DAPI (blue). Scale bar, 200 μm. The apoptosis rate was quantified by SIBIA software. (C)(D) Measurement of caspase-3 activation (n=5). Caspase-3 substrate was used as a positive control. Values are represented as mean ± SD. *P < 0.05 and *P < 0.01 compared with control cells.

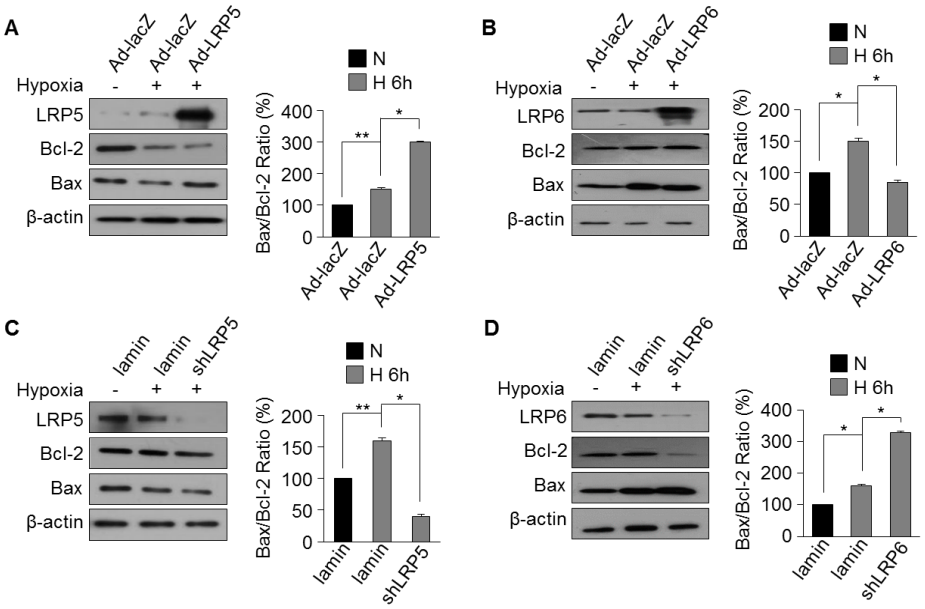

Figure 11. Effect of LRP5 and LRP6 on Bax/Bcl-2 expression under hypoxic condition

Cardiomyocytes were infected with Ad-lacZ, Ad-LRP5/6, lamin or shLRP5/6, respectively, then exposed to normoxia or hypoxia (O_2 1.2%) for 6h. Cells were harvested for western blotting. (A)-(D) Relative expression of Bax and Bcle-2 (n=3). The results are presented as a ratio and converted into the form of a %. Values are represented as mean ± SD. *P < 0.05 and *P < 0.01 compared with control cells.

3.5. Regulation of HIF-1α transcriptional target genes expression by LRP5

Since previous studies have already revealed that silencing of LRP6 promotes cellular damage to ischemic injury [68, 69], this study is focused on elucidating the role and underlying mechanisms of LRP5 in myocardial ischemic injury.

To better understand the mechanism by which LRP5 promotes hypoxia-induced cardiomyocytes death, gene expression profiling was performed using mRNA-seq analysis. First, global gene expression changes due to hypoxia were examined. The scatter plot analysis and differential gene expression (DEG) analysis were identified that 782 genes (>= 2.5-fold change) were upregulated, and 565 genes (=< 0.5-fold change) were downregulated by hypoxic condition (Figure 12A and B). To identify hallmark gene sets enriched among the most upregulated genes, gene ontology (GO) terms and KEGG pathways were performed. As expected, most of GO terms involved the regulation of response to hypoxia, apoptosis, and cell death. Furthermore, KEGG pathways revealed HIF-1α signaling pathway was significantly enriched and upregulated compared to nomoxic cells, indicating that HIF-1α plays an important role in the regulation of proteins for hypoxic adaptation and survival (Figure 12C, details of GO assignment and KEGG analysis are presented in Table 2 and 3).

Next, to determine whether LRP5 regulates HIF-1α signaling under hypoxic condition, Ad-lacZ or Ad-LRP5 infected normoxic or hypoxic cardiomyocytes were subject to mRNA-seq analysis. Heat maps of genes with significant changes (FDR 0.25) in the HIF-1α transcriptional target genes sets that were affected by LRP5 overexpression are shown in Figure 13A. Most of HIF-1α transcriptional

target genes (about 36 genes) expression was downregulated in Ad-LRP5 infected hypoxic cells (Figure 13A and B). To further validate the results of mRNA-seq data, total of 5 representative HIF-1α target genes (Pfkfb3, Nos2, Bnip3l, Glut-1 and EPO) mRNA expression were analyzed by qPCR. Consistent with the mRNA-seq data, the expression of Pfkfb3, Bnip3l, EPO and Glut-1, but not NOS2 and VEGF, were significantly downregulated by LRP5 overexpression, whereas they were markedly upregulated by silencing of LRP5 (Figure 13C). These results demonstrate that LRP5 may modulate the transcriptional activity of HIF-1α, then leading to differential expression of its target genes in hypoxic cardiomyocytes.

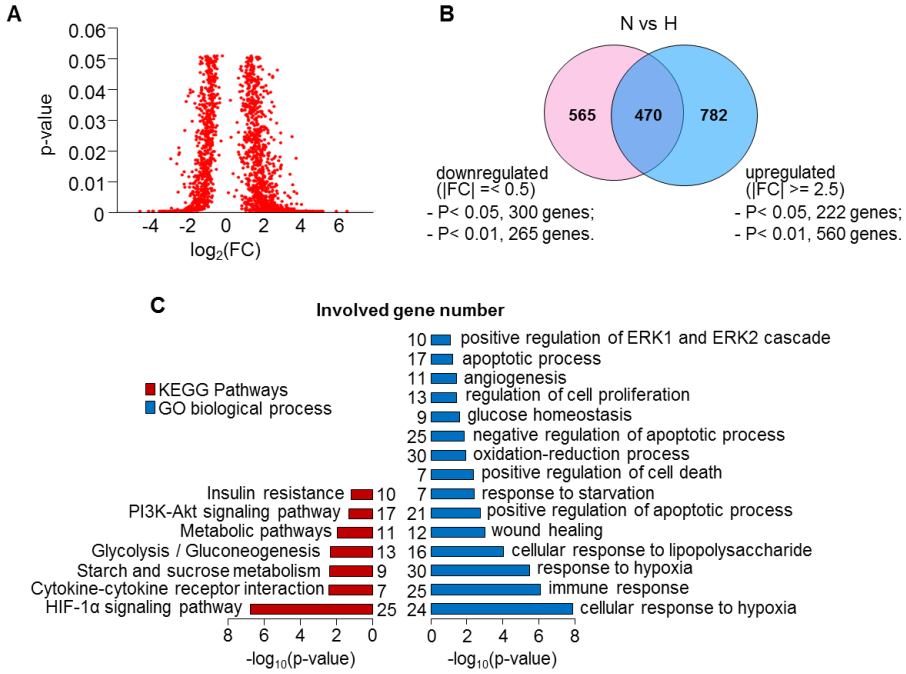

Figure 12. Gene expression changes by hypoxia

Cardiomyocytes were exposed to normoxic or hypoxic condition and extracted for total RNA isolation. Triplicated biological samples were subject to mRNA sequencing. (A) Scatter plot of mRNA seq expression analysis. Scatter plots of transcript expression data for normoxic versus hypoxic condition. The plot is on a log-transformed scale. (B) The number of up and down-regulated DEGs (Normoxia (N) versus Ad-lacZ hypoxia (H), fold change ≥2.5, p-value ≤0.05 or p-value ≤0.01) is shown in Venn diagram. (C) Gene Ontology enrichment analysis in 'Biological Process' category (blue) and KEGG enrichment analysis (red) for genes up-regulated in response to hypoxia. The p-values were calculated using Benjamini-corrected modified Fisher's exact. Details of GO assignment and KEGG analysis are presented in Table 1 and Table 2, respectively.

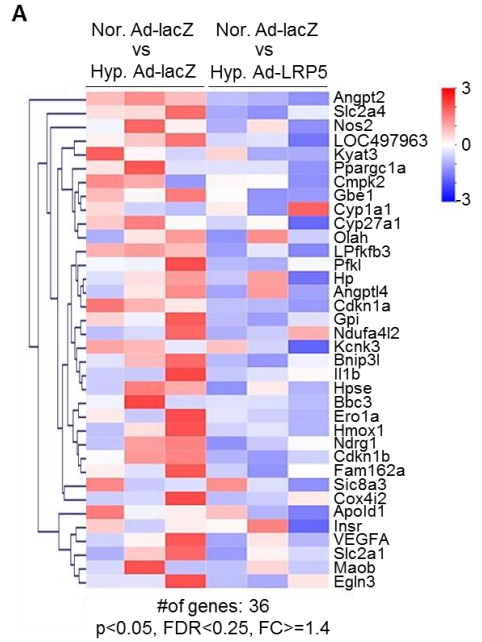

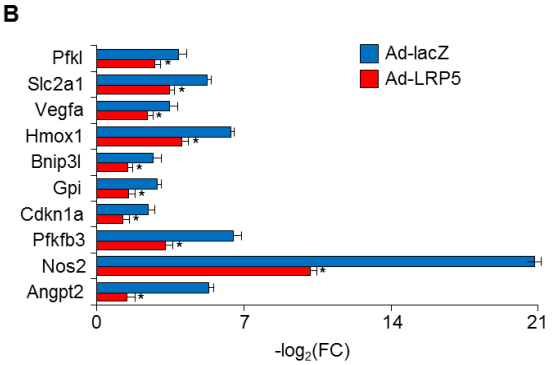

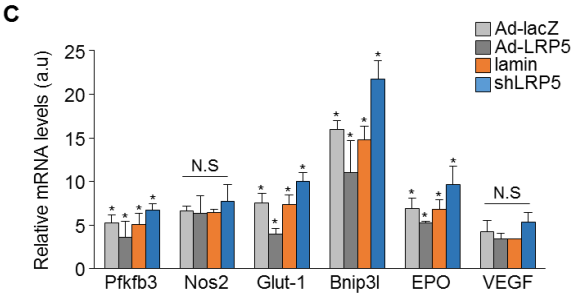

Figure 13. Effects of LRP5 on HIF-1α transcriptional response under hypoxic condition

Cardiomyocytes were exposed to normoxic or hypoxic condition and extracted for total RNA isolation. Triplicated biological samples were subject to mRNA sequencing. (A) Hierarchical cluster analysis of HIF-1α transcriptional target genes between Ad-lacZ and Ad-LRP5-infected hypoxic cardiomyocytes. Each fold change was calculated by normoxic Ad-lacZ control. P<0.05, FDR <0.25, FC>=1.4 (B) The 10 most significantly changed genes between Ad-lacZ and Ad-LRP5-infected hypoxic cardiomyocytes. (C) The qPCR confirmation of mRNA expression of selected genes. Gene expression was normalized to GAPDH. Fold change was calculated by normoxic Ad-lacZ control (n=3). Values are represented as mean ± SD. *P < 0.05 compared with control cells. N.S: non-significant.

Table 2. Functional enrichment analysis of common genes by GO-terms, B.P., biological process

Term	Category	Number of genes	%	p-value	Genes
Cellular response to hypoxia	B.P.	24	2.6	1.3E-08	SLC8A3, TBL2,STC2, IL7, COX4I2, BNIP3, RORA, FOXO3, PPARGC1A, KCNK3, ERO1A, SLC2A4, BBC3, HMOX1, VEGFA, MDM2, FAM162A, NDRG1, MGARP, HIGD1A
Immune response	B.P.	25	3.2	7.8E-07	CSF3, ENPP2, CXCL2, PGLYRP1, OAS3, IFI44L, CXCL6, OAS2, CXCL11, CXCL10, OASL2, RT1-CE10, IL1B, CD24, IL7, RT1-S2, TNFRSF14, C4BPA, TNFRSF9, OAS1I, CXCL13, P2RY14, OAS1B, TGFBR3, OAS1G
Response to hypoxia	B.P.	24	3.1	3.3E-6	PPARA, CYP1A1, EGLN3, APOLD1, BNIP3, EGLN1, HP, CBFA2T3, PPARGC1A, DDIT4, ALDH3A1, EDNRA, CDKN1B, ANG, ABCB1B, HMOX1, VEGFA, TGFBR3, IL1B, KDM3A, CD24, NOS2, ANGPT2, ANGPTL4
Cellular response to lipopolysaccharide	B.P.	16	2.1	0.000092	CYP1A1, GNRH1, MAOB, ACP5, TNFRSF14, HP, CXCL6, STAT1, CCL5, CXCL11, CXCL10, EDNRA, IRAK3, TNFRSF9, CXCL13, KCNJ8, PTGES,ABCB1B, IL1B, NOS2, EIF2AK2
Wound healing	B.P.	12	1.5	0.00098	FNTB, PPARA, ALOX15, HPSE, MAP3K1, ARHGEF19, VEGFA, CXCL2, PDGFRA, IL1B, GRHL3, NOS2
Positive regulation of apoptotic process	B.P.	21	2.7	0.0018	TFAP4, NTF3, BNIP3, EGLN1, FOXO3, BCL2L11, DDIT3, JMY, NTRK3, BBC3, HMOX1, MAP3K1, SCIN, DHODH, IL1B, FAM162A, BCL6, NOS2, EIF2AK2, BMF, TP53INP1
Response to starvation	B.P.	7	0.9	0.0039	HMGCS2, ULK1, PDK4, DHODH, HP, PPARGC1A, DDIT3
Positive regulation of cell death	B.P.	7	0.9	0.0043	CDKN1A, CDKN1B, ACER2, IRF1, IL1B, HP, BCL2L11

Oxidation-reduction process	B.P.	30	3.9	0.012	LOC497963, ALDH1L1, CYB5R2, HSD17B13, EGLN3, EGLN1, CYP4F39, ALDH3A1, CYP39A1, ERO1A, DHODH, KDM3A, SPR, GSTO2, NOS2, KDM5B, HIGD1A, CYP1A1, NDUFA4L2, MAOB, DHDH, DHRS3, LOC102556347, CYP27A1, AKR1C19, AOX1, AOX2, BCO1, CYP2R1
Negative regulation of apoptotic process	B.P.	25	3.2	0.14	MGMT, BNIP3, GLI2, SYCP2, EDNRA, EEF2K, SLC25A27, BCL6, HIGD1A, ANGPTL4, LTK, GNRH1, IL7, PDE3A, BIRC3, DAPK1, IFIT3, ALOX15, CDKN1A, CDKN1B, SYCP3, VEGFA, MDM2, EIF2AK2, SLC40A1
Glucose homeostasis	B.P.	9	1.2	0.025	GPI, SLC2A4, PYGL, PPP1R3G, PDK4, MBD5, PDE3B, FOXO3, INSR
Regulation of cell proliferation	B.P.	13	1.7	0.037	TNFRSF9, CXCL13, CXCL2, IRF1, PLA2G2A, EGLN3, TNFRSF14, BCL6, TXK, CXCL6, NOS2, CXCL11, CXCL10
Angiogenesis	B.P.	11	1.4	0.039	GPI, ANG, HMOX1, VEGFA, APOLD1, PDE3B, ACKR3, CALCRL, RORA, ANGPT2, ANGPTL4
Apoptotic process	B.P.	17	101	0.062	EGLN3, BNIP3, GAS2, FOXO3, BIRC3, NIACR1, DDIT3, DAPK1, DDIT4, TNFRSF9, USP53, BBC3, RNF152, MAPT, IRF1, XAF1, TP53INP1
Positive regulation of ERK1 and ERK2 cascade	B.P.	10	1.3	0.086	EDNRA, ALOX15, C3, SERPINF2, VEGFA, PDGFRA, PLA2G2A, IL1B, ACKR3, CCL5

Table 3. KEGG enrichment analysis of common genes in hypoxic cardiomyocytes

Term	Number of genes	%	p-value	Genes
HIF-1 signaling pathway	32	2.1	1.8E-07	LOC497963, PDK1, PFKFB3, HK2, EGLN3, EGLN1, CDKN1A, CDKN1B, LOC100911625, HMOX1, SLC2A1, VEGFA, ENO2, NOS2, ANGPT2, INSR
PI3K-Akt signaling pathway	20	2.6	0.004	CSF3, IL2RA, IL7, FGF11, FOXO3, BCL2L11, DDIT4, CDKN1A, CDKN1B, COL6A6, COL6A5, VEGFA, PDGFRA, GYS1, MDM2, RELN, GNG4, COL11A2, ANGPT2, INSR
Insulin resistance	10	1.3	0.0043	PPARA, PPP1R3C, PPP1R3B, SLC2A4, PYGL, SLC2A1, GYS1, SLC27A3, INSR, PPARGC1A
Cytokine-cytokine receptor interaction	14	1.8	0.0048	CSF3, IL2RA, IL7, CXCL2, EDA2R, TNFRSF14, ACKR3, CCL5, CXCL11, CXCL10, TNFRSF9, CXCL13, IL15RA, IL1B
Starch and sucrose metabolism	5	0.6	0.011	GPI, GBE1, PYGL, GYS1, HK2
Glycolysis / Gluconeogenesis	6	0.8	0.051	GPI, PFKL, LOC100911625, HK2, ENO2, ALDH3A1
Metabolic pathways	47	6.1	0.063	LOC497963, NAMPT, OLAH, HK2, PPCDC, ALDH3A1, CMPK2, PTGES, HPSE, PLA2G12A, ENO2, DHODH, KYAT1, SPR, KYAT3, NOS2, MTMR7, NADK2, PIK3C2G, CYP1A1, PFKL, NDUFA4L2, ACER2, PIK3C2B, MAOB, COX4I2, AK4, DGKI, LPIN1, GPI, ALOX15, DHRS3, GBE1, CYP27A1, LOC100911625, HMGCS2, LOC102556347, PYGL, AOX1, AOX2, PLA2G2A, MBOAT2, BCO1, PLA2G4F, CYP2R1, PLA2G4B, REV3L

3.6. Effect of LRP5 on HIF-1α expression in hypoxia

Given the above observations, further investigated how LRP5 modulates the transcriptional activity of HIF-1α. To investigate the effect of LRP5 on HIF-1α expression, cardiomyocytes were exposed to normoxic or hypoxic condition and HIF-1α expression was measured by western blotting. As shown in Figure 14A and B, HIF-1α protein levels were rapidly induced within 30min of cellular exposure of hypoxia and reached maximal levels after 1h. As expected, HIF-1α was not detected under normoxic conditions. The HIF-1α expression was markedly reduced in LRP5-overexpressed cardiomyocytes under hypoxia compared with Ad-lacZ treated control cells (Figure 14A), whereas it was enhanced in LRP5-silenced cells (Figure 14B). Together, these findings demonstrated that LRP5 regulates HIF-1α expression under hypoxic condition.

To investigate whether HIF-1α level regulation by LRP5 is regulated at the transcriptional level, HIF-1α mRNA levels were examined using a qPCR. Although the HIF-1α mRNA is constitutively expressed under normoxic conditions (Figure 14C), hypoxia treatment did not result in an increase in mRNA levels (Figure 14D and E). Furthermore, the mRNA level of HIF-1α was not altered by LRP5 overexpression under either normoxic or hypoxic condition (Figure 14D and E). These results indicated that LRP5 does not affect HIF-1α expression at the transcriptional level.

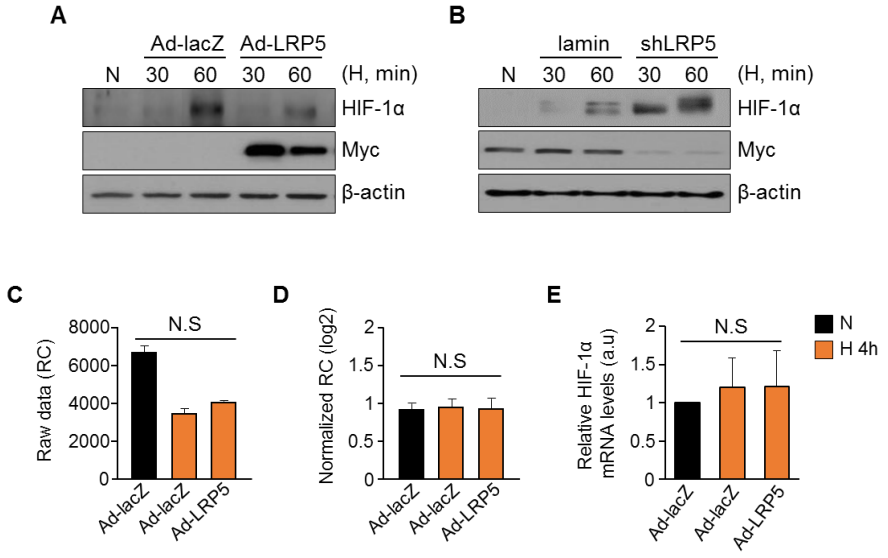

Figure 14. Effect of LRP5 on HIF-1α expression under hypoxic conditions

(A) Ad-lacZ or Ad-LRP5 (B) lamin or shLRP5-infected cardiomyocytes were exposed to either normoxa or hypoxia for 30 and 60 min, and harvest for western blotting. Representative western blot analysis showing HIF-1α protein levels in cardiomyocytes incubated for increasing times under hypoxia (n=4). (C)-(E) Ad-lacZ or Ad-LRP5- infected cardiomyocytes were exposed to either normoxa or hypoxia for 4h and extracted for total RNA isolation. (C) Triplicated biological samples were subject to mRNA sequencing. Raw data (RC) of HIF-1α mRNA in normoxic and hypoxic cardiomyocytes. (D) Each fold change was calculated by normoxic Ad-lacZ control. (E) Transcript levels for HIF-1α were quantified by qPCR analysis (n=4). Gene expression was normalized to GAPDH. Values are represented as mean ± SD. N.S: non-significant.

3.7. Effect of LRP5 on HIF-1α stability

To assess whether LRP5 regulates HIF-1α stability, the HIF-1α half-life was measured after treatment with a global inhibitor of protein synthesis, cycloheximide. HIF-1α-overexpressed cardiomyocytes were treated with cycloheximide (CHX, 50μg/ml) for 2, 5 and 10 min and harvested at various time points for western blotting. As shown in Figure 15, compared with the control condition, LRP5-overexpressed cells reduced the half-life of HIF-1α (half-life of control cells, approximately 4 min; half-life of cells infected with Ad-LRP5, approximately 1.8 min). In contrast, silencing of LRP5 prolonged the half-life of HIF-1α to greater than 10 min. These date showed that LRP5 regulates HIF-1α expression by decreasing protein stability in cardiomyocytes.

For transactivation of HIF-1α, HIF-1α must translocate into the nucleus. Nuclear extracts from cardiomyocytes exposed to hypoxia increased translocation of HIF-1α and silencing of LRP5 further enhanced hypoxia-induced nuclear translocation of HIF-1α. Whereas, overexpression of LRP5 dramatically attenuated nucleus translocation of HIF-1α compared to control cells (Figure 16A). Moreover, immunocytochemistry demonstrated higher levels of HIF-1α staining in the nucleus in LRP5-silenced hypoxic cardiomyocytes than lamin control cells (Figure 16B). To further examine the role of LRP5 in regulating HIF-1α transcriptional activity, gene reporter assay was performed using a luciferase reporter plasmid driven by three HRE (Hypoxia-Responsive Element) sequences. As shown in Figure 16C, exposure of LRP5-infected cells to hypoxic conditions decreased HRE reporter activity as compared with Ad-lacZ control cells, and that activity was higher in shLRP5-infected hypoxic cardiomyocytes

(Figure 16D). Taken together, these results demonstrate that LRP5 negatively regulates HIF-1α stability, which in turn inhibits HIF-1α transcriptional activity.

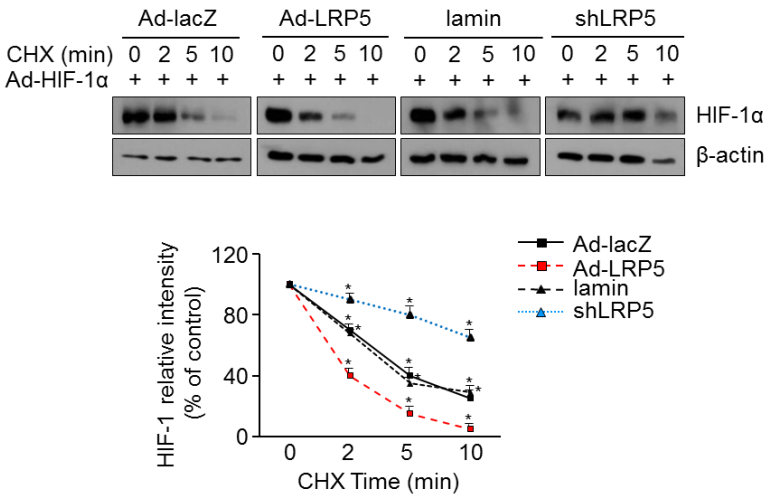

Figure 15. Effect of LRP5 on HIF-1α half-life

Representative western blot analysis is showing HIF-1α half-life in cardiomyocytes. Cardiomyocyte were co-infected with Ad-HIF-1α and Ad-lacZ, Ad-LRP5 or shLRP5, respectively. The cells were treated with CHX (50μg/ml) for indicated time periods before being harvested for western blotting (n=4). Protein levels were normalized to β-actin levels. Values are represented as mean ± SD. *P < 0.05 compared with each control cells without CHX.

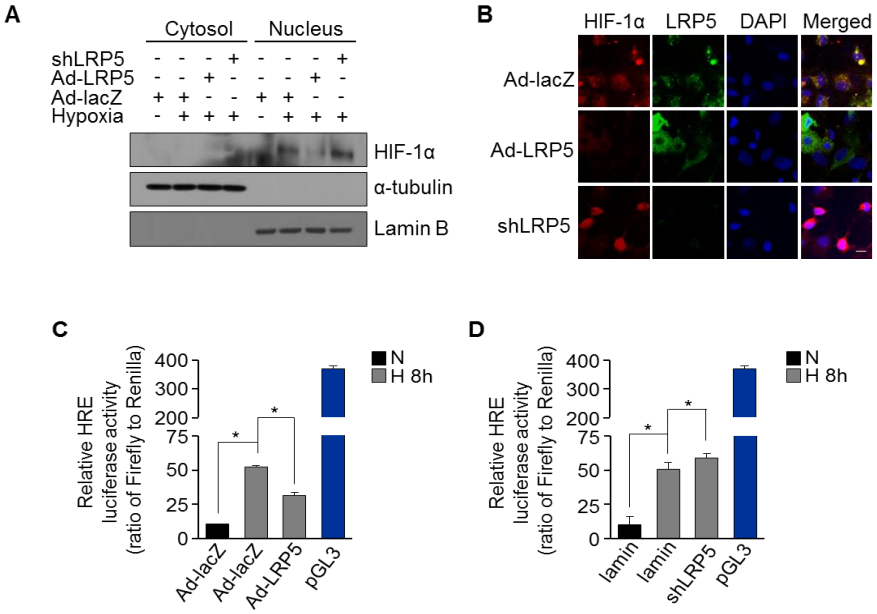

Figure 16. Effect of LRP5 on nuclear translocation of HIF-1α and HRE reporter activity

(A) Nuclear translocation of HIF-1α in Ad-lacZ, Ad-LRP5 or shLRP5 expressed cardiomyocytes; α-tubulin and lamin B were used for cytoplasmic and nuclear protein controls, respectively (n=4). (B) Ad-lacZ, Ad-LRP5, lamin or shLRP5 infected cardiomyocytes were stained with HIF-1α (red) and counterstained with DAPI (blue) after exposed to normoxic or hypoxic condition, respectively (n=3). The image showed translocation of HIF-1α in nucleus. Scale bar, 200 μm. (C)(D) Transactivation of HRE-luciferase activity. Cardiomyocytes were co-transfected with HRE luciferase reporter and pRL-TK vector (control for transfection efficiency) along with (C) Ad-lacZ or Ad-LRP5 (D) lamin or shLRP5 infection. The pGL3 promoter vector was used for positive control. Relative luciferase activity were the ratio of luciferase over renilla activity (n=3). Values are represented as mean ± SD. *P < 0.05 compared with control cells.

3.8. Regulation of HIF-1α stability by LRP5 via ubiquitin-proteasome pathway

To examine whether LRP5 induced HIF-1α destabilization is mediated by the proteasome degradation pathway, cardiomyocytes were treated with proteasome inhibitor MG132 for 6 h and exposed to hypoxia for 1h. As shown in Figure 17, the degradation of HIF-1α with LRP5 overexpression was completely restored by MG132. These results indicated that LRP5 aggravates HIF-1α stability through the ubiquitin-proteasome pathway under hypoxic condition.

3.9. Effect of LRP5 on hydroxylation of HIF-1α

PHDs (PHD1-3) serve as cellular oxygen sensors to regulate HIF-1α stabilization by controlling its prolyl-hydroxylation (at Pro402 and Pro564) modification [47, 50, 78]. To examine whether LRP5-midiated destabilization of HIF-1α occurs through PHDs regulation, the hydroxylated levels of HIF-1α (Hyp564) was assessed using a specific antibody for the hydroxylated form of the protein (Pro564). As shown in Figure 18A, hydroxylated levels of HIF-1α (Pro564) was significantly suppressed by more than 80% within 30 minutes under hypoxia, but LRP5-overexpressed cells showed an unaltered levels of HIF-1α hydroxylation compared to hypoxic Ad-lacZ cells. Moreover, PHD activity was significantly increased in LRP5-overexpressed cardiomyocytes under hypoxia with time dependent manners; whereas LRP5-silenced cells exhibited the significant decrease of PHD2 activity compared with Ad-lacZ control cells (Figure 18B). Together, the treatment of dimethyloxalylglycine (DMOG), an inhibitor of PHDs, before hypoxia was significantly restored the loss of cell

viability (Figure 18C). These results demonstrate that LRP5 play a crucial role in regulating the hydroxylation of HIF-1α mediated by PHDs.

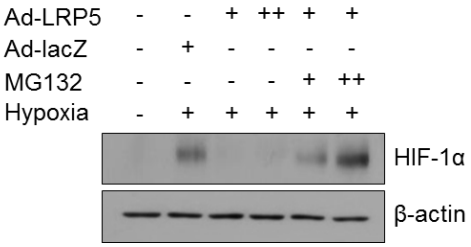

Figure 17. Effect of LRP5 on the ubiquitin-proteasome system

Cardiomyocytes were infected with Ad-lacZ or Ad-LRP5. 48h after adenovirus infection, cells were exposed to normoxia or hypoxia for 1h in the absence or presence of 10μM MG132 as indicated. HIF-1α levels were detected by western blotting (n=4). Protein levels were normalized to β-actin levels.

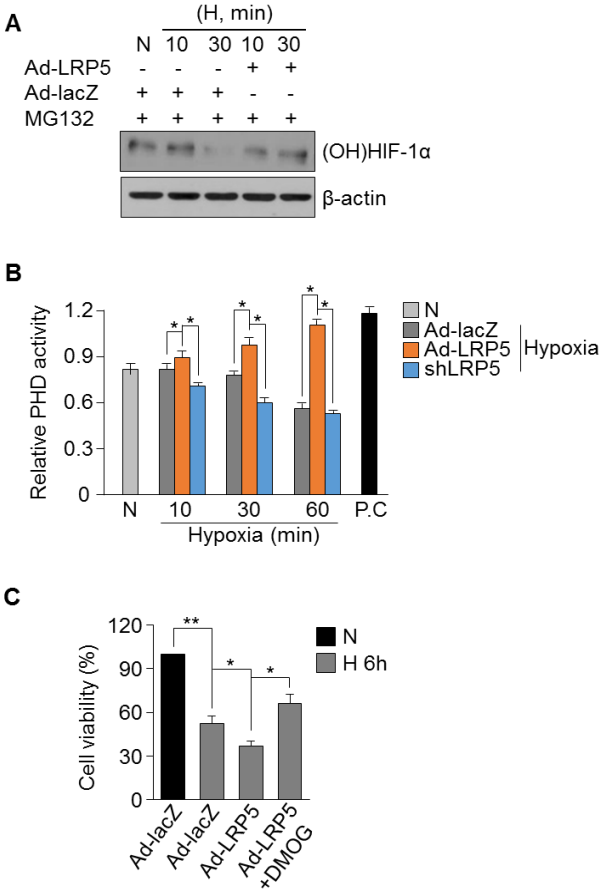

Figure 18. Effect of LRP5 on PHD2 activity

(A) Cardiomyocytes were infected with the indicated adenoviruses. 48h after adenovirus infection, cells were treated with 10μM MG132 for 6h and exposed to hypoxia for 10min or 30min. The levels of hydroxylated HIF-1α were determined a specific antibody recognizing Pro564-HIF-1α (n=4). (B) Biotinylated HIF-1α oxygen-dependent degradation domain and a hydroxylated control peptide were detected using a TMB substrate at 650nm (n=4). (C) Effect of DMOG on cell viability. The cell viability was determined by MTT assay (n=3). Values are represented as mean ± SD. *P < 0.05 and *P < 0.01 compared with control cells

3.10. Identification of LRP5 as a specific PHD2 interactor

To assess which PHDs involved in LRP5-mediated hydroxylation of HIF-1α, examined mRNA levels of PHDs under hypoxic condition. Both PHD2 and PHD3 significantly were upregulated by hypoxia, but not PHD1 (data not shown). To further investigate whether LRP5 physically interacts with PHDs, co-immunoprecipitation experiment was performed. As shown in Figure 19A, LRP5 showed specific interaction with endogenous PHD2 only, confirming that PHD1 and PHD3 did not co-immunoprecipitated.

To further confirm the LRP5:PHD2 interaction, cardiomyocytes were co-expressed Myc-tagged LRP5 and PHD2 and performed immunoprecipitation analyses. When cell lysates were immunoprecipitated with anti-PHD2 antibody, Myc-LRP5 was successfully coimmunoprecipitated (Figure 19B). Reciprocally, PHD2 was co-imunoprecipitated when cell lysates were immunoprecipitated with anti-Myc antibody (Figure 19C). Taken together, the interaction between LRP5 and PHD2 was attenuated in Ad-lacZ control cells under hypoxia, which was augmented in LRP5-overexpressed cardiomyocytes followed by hypoxia (Figure 19D). Since it is well known that PHD2 interact with HIF-1α, next confirmed the effects of LRP5 expressions on the molecular association between HIF-1α and PHD2. Consistently, the levels of coimmunoprecipitated HIF-1α by anti-PHD2 antibody was increased in LRP5-overexpressed cells under hypoxic condition, whereas decreased in LRP5-silenced cells (Figure 19E). The hydroxylated levels of HIF-1α was significantly enhanced with PHD2 overexpression in LRP5-overexpressed cardiomyocytes compared with Ad-lacZ control cells, but not in LRP5-silenced cells (Figure 19F). Interestingly, although LRP5 and LRP6 are highly homologous, LRP6 did not interact with PHD2 (Figure 20).

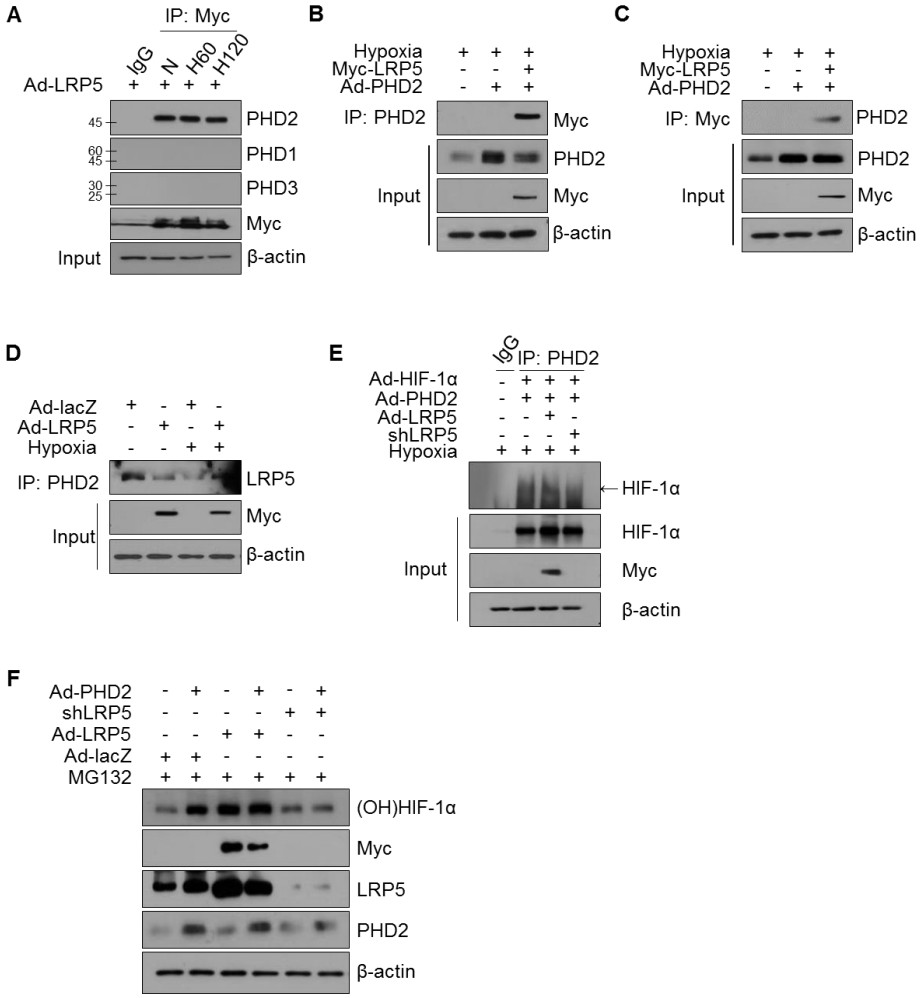

Figure 19. LRP5 interacts with PHD2 in cardiomyocytes

(A) Cardiomyocyte were infected with Ad-LRP5 and exposed to hypoxia for 60min or 120min, respectively. Whole-cell lysate were subjected to immunoprecipitation using an anti-Myc antibody followed by western blotting using antibodies indicated to the right of the blot (n=4). (B) Myc-tagged Ad-LRP5 and Ad-PHD2 were co-infected into cardiomyocytes and exposed to hypoxia. After 90min, whole-cell lysate were subjected to immunoprecipitation using an anti-PHD2 antibody followed by western blotting using the anti-Myc and anti-PHD2 antibodies (n=4). (C) Cardiomyocytes were prepared as in (B), and lysates were subjected to immunoprecipitation using an anti-Myc antibody followed by western blotting using the anti-Myc and anti- PHD2 antibodies (n=4). (D) Cardiomyocyte were infected with Ad-lacZ or Ad-LRP5, respectively, and exposed to with or without with hypoxia. After 90min, whole-cell lysate were subjected to immunoprecipitation using an anti-PHD2 antibody followed by western blotting using the anti-LRP5. (E) Cardiomyocytes were co-transfected with adenoviruses as indicated and exposed to hypoxia. After 90min, cell lysates were subjected to immunoprecipitation using an anti-PHD2 antibody followed by western blotting using the indicated antibodies (n=3). IgG was used as a negative control, and β-actin was used as a loading control. (F) Ad-lacZ, Ad-LRP5 or shLRP5-infected cardiomyocytes, with or without co-infected with Ad-PHD2 were exposed to hypoxia for 30 min. The levels of hydroxylated HIF-1α were determined a specific antibody recognizing Pro564-HIF-1α (n=4).

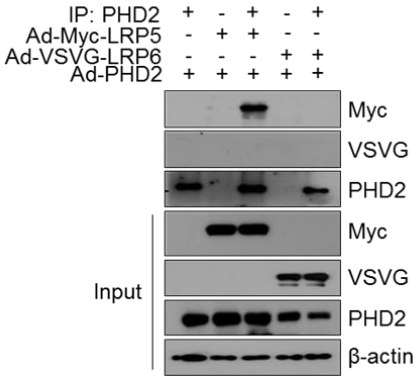

Figure 20. LRP6 does not interact with PHD2 in cardiomyocytes

Cardiomyocytes were co-transfected with adenoviruses as indicated and cell lysates were subjected to immunoprecipitation using an anti-PHD2 (IP: +) antibody or IgG (IP: -) followed by western blotting using the indicated antibodies (n=3). IgG was used as a negative control, and β-actin was used as a loading control.

3.11. Wnt/β-catenin signaling-independent role of LRP5 in regulating HIF-1α stability

LRP5 is known as a Wnt co-receptor for transduce canonical Wnt/β-catenin signaling pathway. LRP5 phosphorylated by the Wnt ligands inhibits glycogen synthase kinase-3β (GSK-3β) phosphorylation by recruiting axin, scaffolding protein, then, β-catenin is stabilized in cytoplasmic and translocate into the nucleus [8, 19]. To investigate the effect of acute hypoxia on Wnt/β-catenin signaling, the alteration of β-catenin expression was confirmed according to hypoxia induction time. As shown in Figure 21A, the expression of β-catenin was not significantly changed at any time point of hypoxia treatment. Supporting this, mRNA levels of β-catenin, axin2, and wnt3a, direct Wnt/β-catenin target genes, showed any significant alterations under hypoxic conditions (Figure 21B).

Next, to examine whether LRP5 regulates Wnt/β-catenin signaling under hypoxic condition, β-catenin expression were assessed. As shown in Figure 22A, silencing of LRP5 did not change β-catenin expression but silencing of LRP6 was downregulated expression of β-catenin. Furthermore, the overexpression or silencing of LRP5 did not affect β-catenin expression, both in the cytoplasm and nucleus (Figure 22B). The mRNA levels of Wnt/β-catenin target genes also did not altered by LRP5 regulation (Figure 22C). These results suggest that acute hypoxia does not activate Wnt/β-catenin signaling, and the regulation of HIF-1α stability by LRP5 is independent of Wnt/β-catenin signaling pathway.

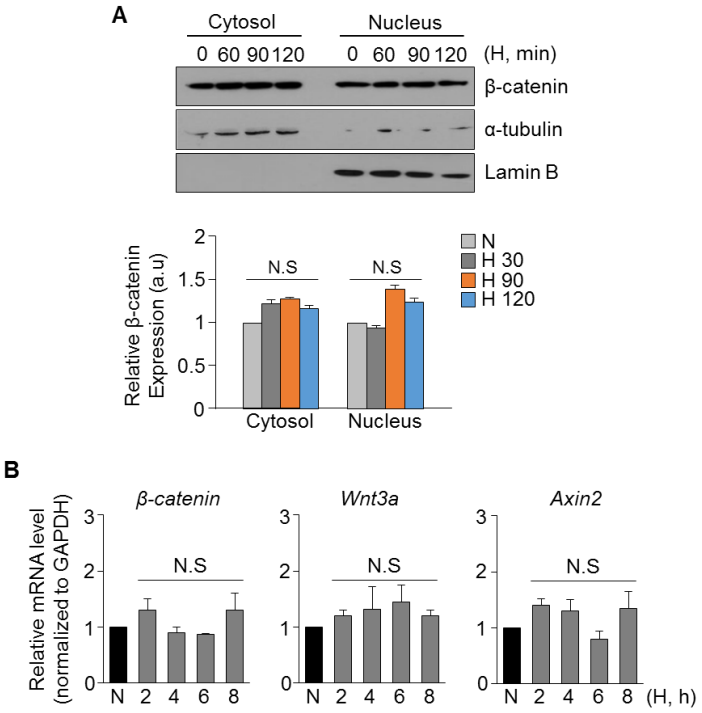

Figure 21. The effect of hypoxia on Wnt/β-catenin signaling pathway

(A) Cardiomyocytes were exposed to normoxia or hypoxia and harvested at the indicated time points for western blotting. The α-tubulin and lamin B were used for cytoplasmic and nuclear protein controls, respectively (n=4). The cytosol expression was normalized by α-tubulin, and the nucleus expression was normalized by lamin B. (B) The mRNA expression of β-catenin, Wnt3a and Axin2 were quantified by qPCR analysis (n=4). Gene expression was normalized to GAPDH. Values are represented as mean ± SD. N.S: non-significant.

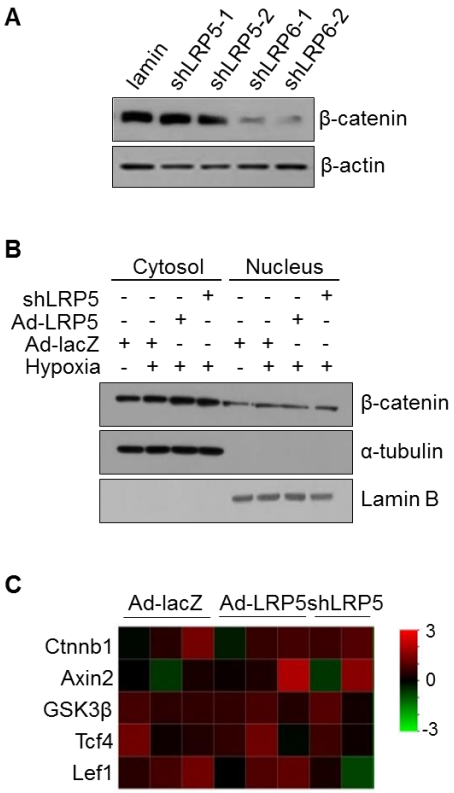

Figure 22. LRP5 regulates HIF-1α stability independent of Wnt/β-catenin signaling pathway.

(A) Cardiomyocytes infected with lamin, shLRP5 or shLRP6, respectively and harvested for western blotting (n=3). (shLRP5/6-1: 20 of MOI, shLRP5/6-2: 40 or MOI). (B) Nuclear translocation of HIF-1α and β-catenin in Ad-lacZ, Ad-LRP5 or shLRP5 expressed cardiomyocytes; α-tubulin and Lamin B were used for cytoplasmic and nuclear protein controls, respectively (n=4). (C) Hierarchical cluster analysis of Wnt/β-catenin signaling-related genes. Each fold change was calculated by normoxic Ad-lacZ control. Values are represented as mean ± SD. *P<0.05

3.12. Effect of LRP5 phosphorylation on hypoxia

To investigate the effect of LRP5 phosphorylation in hypoxia, phosphorylation of LRP5 was assessed under hypoxic condition. As shown in Figure 23, the exposure of hypoxia dramatically reduced the phosphorylation levels of LRP5 at Ser1503 (the first PPP[S/T]P motif in ICD; intracellular domain) with time-dependent manner but did not altered phosphorylation levels of LRP5 at Thr1492 (S/T cluster in ICD). The significant reduction of the phosphorylated levels at Ser1503 by hypoxia has been observed within 30 min and complete reduction at 60min. In the above results, protein level of LRP5 was increased in hypoxic conditions at 8 hours (Figure 7B), and the regulation of HIF-1α stability by LRP5 occurred within 1 hours, suggesting that the alteration of phosphorylated levels, not expression levels, of LRP5 might be a signaling trigger for regulating HIF-1α stability under hypoxia in cardiomyocytes.

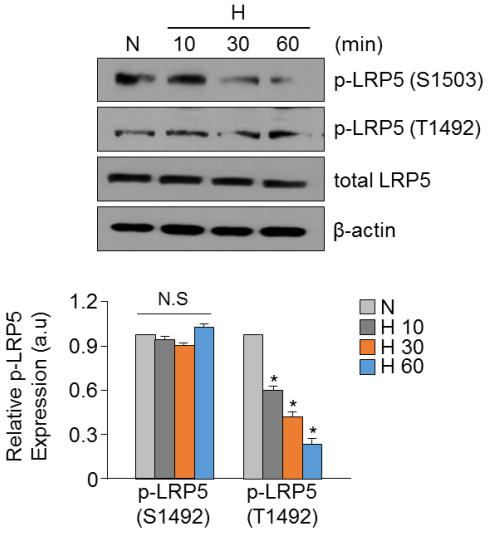

Figure 23. Hypoxia induces phosphorylation of LRP5 at S1503

Cardiomyocytes were exposed with the indicated hypoxic times. The expression levels of p-LRP5 (S1503) and p-LRP5 (T1492) were analyzed by western blotting (n=5). Protein levels were normalized to total LRP5 levels. Values are represented as mean ± SD. *P < 0.05 compared with normoxia.

3.13. Effect of LRP5 phosphorylation on HIF-1α stability

For this hypothesis, next made adenoviral constructs mutated the each of S/T cluster and five PPP(S/T)P phosphorylation motifs (T1492D, S1503A, T1541D, T1578D, S1598A, and S1609A) in LRP5 ICD and examined the effects of each constructs on the expression of HIF-1α (Figure 24A). Adenoviral vector for mutants (named as △1~△6) were successfully constructed for infection into cardiomyocytes using a sequencing analysis (data not shown). To determine the role of LRP5 phosphorylation in stability of HIF-1α, cardiomyocytes were infected with adenoviruses as shown in Figure 23B, and exposed to hypoxia for 90 min. The expression of HIF-1α was significantly decreased when infected with Ad-LRP5 compared with Ad-lacZ hypoxic cells, and those decreased level of HIF-1α was prevented by T1492D (△1), S1503A (△2) and T1541D (△3) mutants but not by T1578D (△4), S1598A (△5)and S1609A (△6) mutants (Figure 24B). The △1 and △2 almost completely restored HIF-1α expression by LRP5 overexpression, and △3 had a slight effect. These data showed that the regulation of HIF-1α stability by LRP5 is regulated by its phosphorylation.

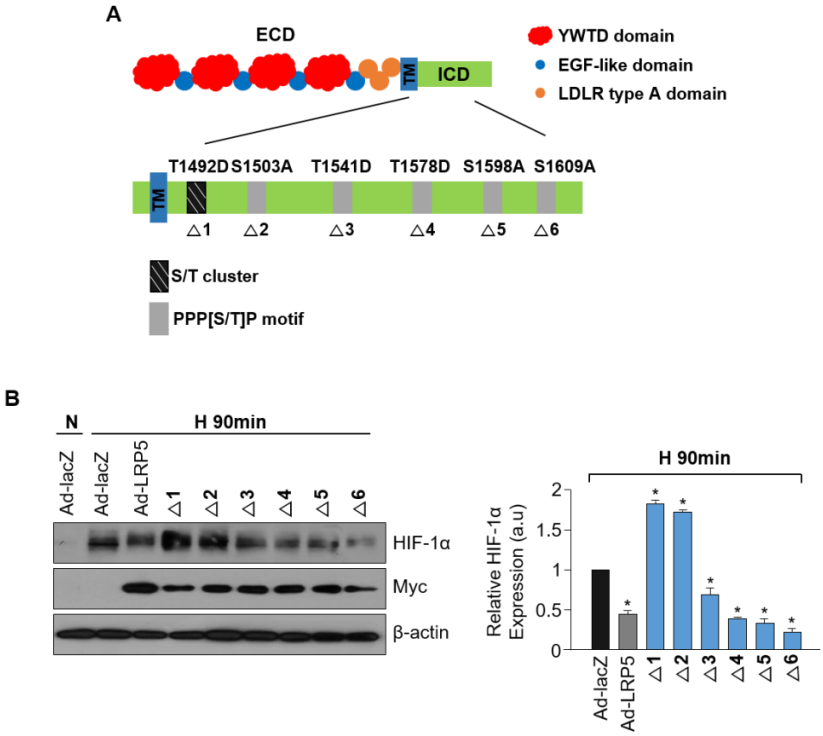

Figure 24. Effect of LRP5 mutations on HIF-1α expression

(A) Schematic diagram of LRP5 phosphorylation site mutations. (B) Cardiomyocytes were infected with the indicated adenoviruses. 48h after adenovirus infection, cells were exposed to hypoxia for 90min. The expression levels of HIF-1α were analyzed by western blotting (n=3). Protein levels were normalized to β-actin levels. Values are represented as mean ± SD. *P < 0.05 compared with hypoxic Ad-lacZ cells.

3.14. Adenoviruses injection into heart

Considering the above results, we further analyzed functional effects of LRP5 in myocardial injury *in vivo*. First, adenoviruses expressing lacZ, LRP5, lamin and shLRP5 were injected into the free walls of the left ventricle of rats, and then the rats were subjected to ischemia/reperfusion injury (I/R injury) on 3 days after injection. X-gal staining, immunohistochemistry and western blotting analysis were performed 3 days after the infection of the adenoviruses. As shown in Figure 25A and B, adenoviral gene delivery was successful using X-gal staining for β–galactosidase activity in the Ad-lacZ injected heart tissues and the immunohistochemical staining of LRP5 using an anti-Myc antibody. In addition, immunoblot showed successfully silenced-endogenous LRP5 expression in shLRP5-injected cardiac tissue compared to lamin control cardiac tissue (Figure 25C).

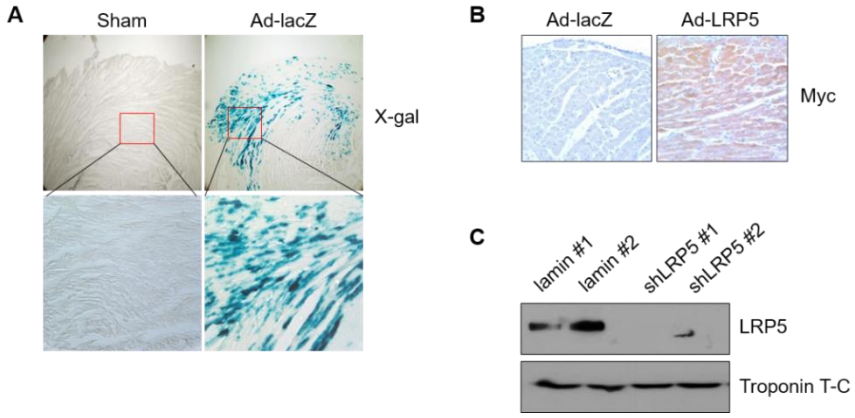

Figure 25. *In vivo* myocardial gene delivery using adenoviruses

Hearts were harvested from sham-operated or adenoviruses-injected rat. (A) Representative sections from Sham or Ad-lacZ-injected heart tissues stained with X-gal (blue) for assess β-galactosidase activity (n=3) (B) Representative immunohistostaining images of Ad-lacZ or Ad-LRP5-infected heart sections using an anti-myc antibody (n=3). (C) Representative immnoblot image of lamin or shLRP5-infected heart lysates (n=3). Troponin T-C was used as the loading control.

3.15. Effect of LRP5 on I/R-induced cardiac injury in *in vivo*

To further measure the cardiac function by LRP5 regulation, hemodynamic assessment was performed using a Millar catheterization. Each group rats were subjected to ischemia for 60 min followed by reperfusion for 2 weeks. Hemodynamic analyses revealed that LRP5 overexpression (LRP5-MI) MI groups displayed a higher end-diastolic pressure-volume relationship (EDPVR) slope (Figure 26A), and deterioration in cardiac function as evidenced by decreased ejection fraction (EF), increased blood pressure, and reduction in the maximal rate of the decrease in left ventricular pressure (-dp/dt) compared to lacZ-MI models (Figure 26B). Conversely, LRP5-silenced MI groups (shLRP5-MI) showed significant improvements in EDPVR slope, EF, blood pressure, dp/dt rates compared to lamin-MI (Figure 26A and B).

Infarct area in heart tissue was measured with TTC staining. As shown in Figure 27, smaller infarct size was observed in shLRP5-MI heart, whereas LRP5-MI heart showed increased infarct size compared with lacZ-MI control heart. These results demonstrate that silencing of LRP5 prevented I/R-induced cardiac injury.

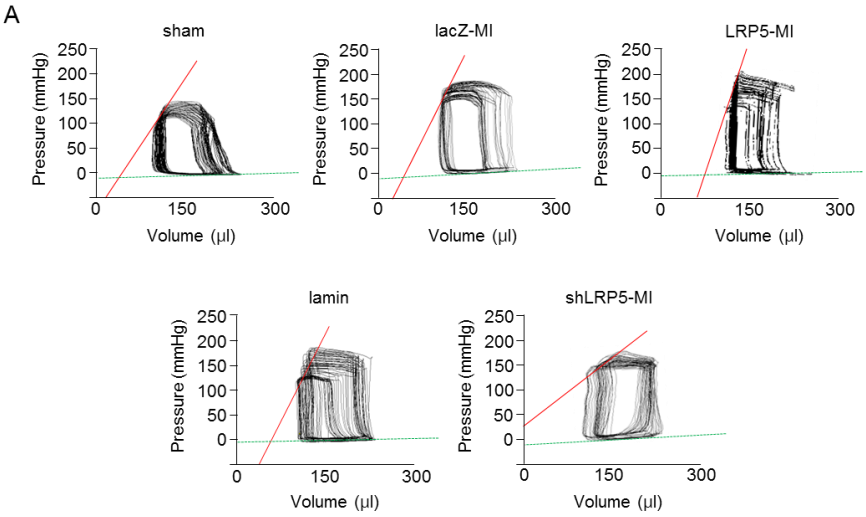

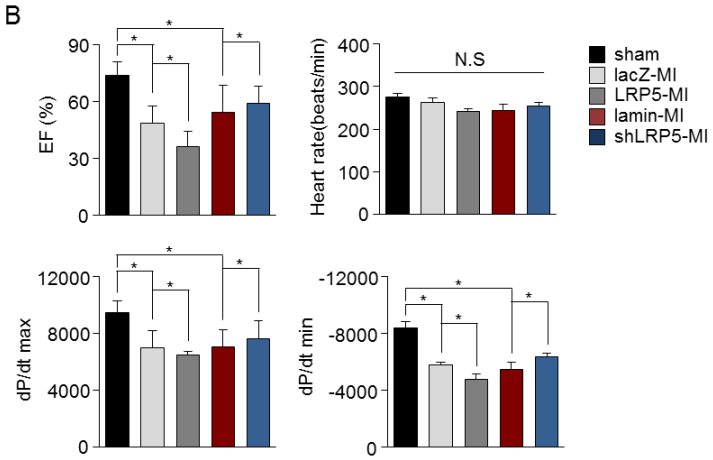

Figure 26. Hemodynamic assessment of LRP5-overexpressed and silenced I/R-induced hearts

(A) A representative image of pressure-volume loop analysis. (B) Statistical analysis of the results of hemodynamic analysis, including ejection fraction (EF), heart rate, dp/dt max (maximal rate of pressure increase) and -dp/dt min (maximal rate of pressure decrease) in each group (n= 4-9 rats per experimental group). Values are represented as mean ± SD. *P < 0.05 compared with lacZ-MI and lamin-MI.

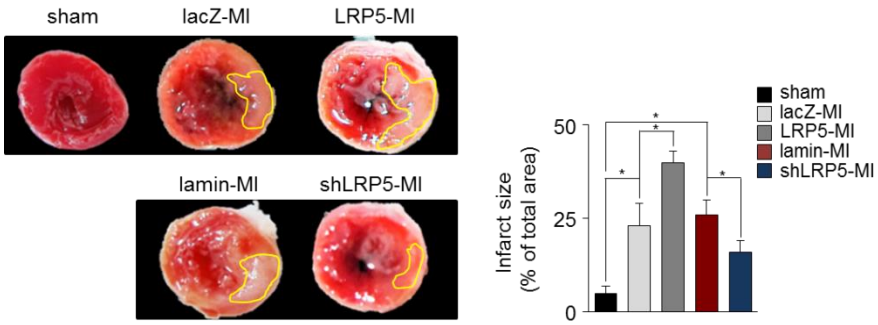

Figure 27. Determination of myocardial infarct size in *in vivo*

Representative photographs of TTC-stained myocardium sections from LRP5-overexpressed or LRP5-silenced I/R-induced hearts. LV infarct size (white areas) is presented as percent of total ventricular area (n=3 rats per experimental group). Values are represented as mean ± SD. *P < 0.05 compared with lacZ-MI and lamin-MI.

3.16. Effect of LRP5 on myocardial fibrosis in I/R injury

Cardiac fibrosis is a commonly observed process in most cardiac pathologies, including the remodeling process following myocardial infarction [79]. To determine the effect of LRP5 on myocardial fibrosis induced by I/R, Masson's trichrome staining were performed. As shown in Figure 29, shLRP5-MI group significantly reduced LV (left ventricle) fibrosis score and percentage area of fibrosis in the LV at 3 weeks following I/R injury. Conversely, LRP5-MI group more increased fibrosis compared with lacZ-MI (Figure 28). These data suggest that silencing of LRP5 can reduce cardiac fibrosis in I/R-injured heart model.

3.17. Effect of LRP5 on HIF-1α expression in I/R injury

To identify the expression of HIF-1α in the LRP5-regulated MI model, immunohistochemistry was performed. As shown in Figure 29, the expression level of HIF-1α were positively and negatively, correlated with the levels of LRP5 in I/R-injured myocardium. Taken together, this study suggests that LRP5 regulates HIF-1α stability in ischemic myocardium via the interaction with PHD2.

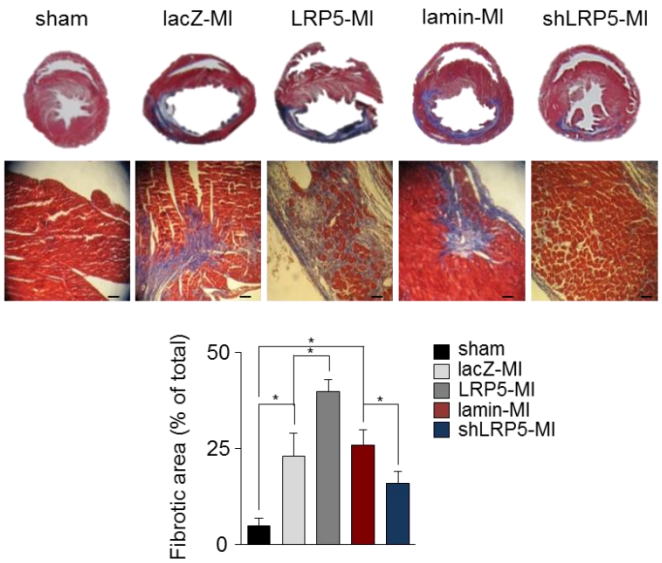

Figure 28. Determination of myocardial fibrosis in I/R models

Representative Masson's trichrome staining images after 2week I/R operation. Quantification expressed as a percentage of fibrosis from the total area (n=3-5 rats per experimental group). Scale bar, 100 μm. Values are represented as mean ± SD. *P < 0.05 compared with lacZ-MI and lamin-MI.

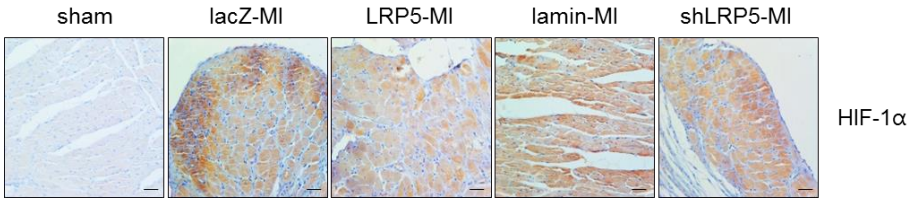

Figure 29. Determination of HIF-1α expression in I/R models

Representative images of immunohistochemical staining for HIF-1α in LRP5-overexpressed or LRP5-silenced I/R-induced hearts (n=3-5 rats per experimental group). Scale bar, 100 μm.

4. Discussion

Hypoxia is associated with various pathologic conditions including myocardial infarction (MI). Despite improvements in the diagnosis and treatment for cardiac pathologies, MI remains the leading cause of death and disability worldwide. Here, this study identified previously unknown Wnt/β-catenin signaling-independent function of LRP5 in regulating PHD2-mediated HIF-1α stability in ischemic myocardium. Several lines of evidence support our conclusions. LRP5 expression is significantly increased in hypoxia-induced cardiomyocytes. LRP5 destabilizes HIF-1α by interacting with PHD2 and this leads to suppression of transcriptional target genes of HIF-1α. Furthermore, the LRP5-dependent regulation of HIF-1α stability is independent of Wnt/β-catenin signaling, it is mediated by phosphorylations of LRP5. Importantly, silencing of LRP5 protects against I/R induced myocardial infarction.

In this study, LRP5 and LRP6 showed opposite expression patterns and function in hypoxia-induced cardiomyocytes. LRP5 and LRP6 are structurally similar, and these two receptors have been proposed to function similarly in the same contexts and signaling pathways. However, recent studies highlighted that they display clearly distinct functions [17]. For example, numerous of studies have indicated that LRP6 is more critical than LRP5 in developmental processes. Although LRP5 is expressed during embryogenesis, $Lrp5^{-/-}$ mice are viable and do not show any developmental abnormality, whereas, $Lrp6^{-/-}$ mice die at birth [80, 81]. Moreover, LRP6 appears to be crucially important for glucose and lipid metabolism signaling [15, 72], while LRP5 plays a more important role in bone-mass phenotype [80, 82]. Another remarkable point of difference between LRP5 and LRP6 function is that the affected Wnt signal activation might be different,

although both LRP5 and LRP6 are known as Wnt co-receptor. Similarly in mammalian cell culture, LRP5 only weakly activates the Wnt signaling in the absence of an exogenous Wnt ligans, in contrast to the highly active LRP6 [9, 83]. These results are consistent with genetic studies that LRP6 appears to be the stronger of the two receptors in the Wnt pathway. Indeed, our results also identified that only silencing of LRP6 in cardiomyocyte was implicated in downregulation of β-catenin expression (Figure 22A); indicating LRP6 is more effective transducer of Wnt activation.

Wnt signaling has diverse functions in cardiac development, homeostasis and repair process [19]. It is usually silent in the normal adult myocardium and reactivated after experimental MI injury in various animal models. Cardiomyocte-specific deletion of β-catenin or secreted frizzled-related proteins sFRP1 and sFRP2-based Wnt antagonism has been demonstrated improved cardiac function, reduced infarct size, inhibition of fibrosis and neutrophil infiltration [64, 65, 84-86]. In MI, injection of DKK2, an antagonist of Wnt signaling that binds to the LRP5 and LRP6, was shown to be beneficial for infarct healing in a cardiac ischemia/reperfusion model, as it reduced infarct size at 1 week post-MI and improved function at 3 weeks post-MI. As shown in Figure 21 and 22, β-catenin level did not changed at low O_2 levels (1.2%) and short time exposures (30-120 min), indicating that the Wnt/β-catenin signaling is not affected by acute hypoxic condition. Because Wnt signaling activated during the remodeling process such as wound healing following MI. These Wnt signaling activation is showed in many cell types including fibroblasts, progenitor cells and endothelial cells in addition to cardiomyocytes [87]. The activation pattern followed the expression pattern of multiple Wnt signaling-related genes, with an increase in the 1 week after MI and

a gradual decrease after the 2 weeks. Therefore, Wnt signaling activation occurs during infarct healing in inflammation, fibrosis and neovascularization [88].

The transcription factor HIF-1α plays a crucial role in acute and long-term adaptive physiological cellular responses to hypoxia by activating the transcriptional target genes such as the metabolic swich to glycolysis, growth factor, migration, autophage, inflammation and apoptosis, as well as genes encoding erythropoiesis [56]. HIF-1α activation in ischemic hearts has been considered a target for therapeutic strategies. In this study were examined the effect of LRP5 on the expression of HIF-1α target genes using an mRNA-seq analysis and qPCR, and found that LRP5 repressed their expression in hypoxic cardiomyocytes (Figure 13A-C). Moreover, the data showed that LRP5 negatively regulates HIF-1α stability but not affects HIF-1α expression at the transcriptional level (Figure 14). As shown in Figure 14C, HIF-1α mRNA is constitutively present in normoxic conditions, hypoxia is not known to modify HIF-1α mRNA levels [51]. The half-life of the HIF-1α is extremly short because it is rapidly degraded in normoxic coditions, indicating that the protein content of HIF-1α is regulated by changes in tis rate of degradation.

In mammals, there are 3 isoforms of PHDs (termed PHD1-3) and PHD2 and PHD3 are known to be highly expressed in the heart [53]. Particularly, PHD2 is known as main HIF-1α modulating in heart. These results also observed that both PHD2 and PHD3 significantly were upregulated under hypoxic condition but not PHD1 (Figure 19).

Because tumor hypoxia and activation of HIF-1α affect most of the cancer hallmarks; our investigation in turn would be greatly useful for future application for tumor therapeutic studies. So it will be of interest to investigate the impact of LRP5 on HIF-1α levels and expression of HIF-1α downstream genes in

various cancer cells, which should be addressed by future experiment. In conclusion, this study showed here that an important role for LRP5 is as a novel regulator of HIF-1α stability under hypoxic condition in cardiomyocytes.

5. References

[1] G.L. Semenza, Hypoxia-inducible factor 1: master regulator of O2 homeostasis, Curr Opin Genet Dev, 8 (1998) 588-594.

[2] A.L. Harris, Hypoxia--a key regulatory factor in tumour growth, Nat Rev Cancer, 2 (2002) 38-47.

[3] R.S. Velagaleti, M.J. Pencina, J.M. Murabito, T.J. Wang, N.I. Parikh, R.B. D'Agostino, D. Levy, W.B. Kannel, R.S. Vasan, Long-term trends in the incidence of heart failure after myocardial infarction, Circulation, 118 (2008) 2057-2062.

[4] F. Van de Werf, J. Bax, A. Betriu, C. Blomstrom-Lundqvist, F. Crea, V. Falk, G. Filippatos, K. Fox, K. Huber, A. Kastrati, A. Rosengren, P.G. Steg, M. Tubaro, F. Verheugt, F. Weidinger, M. Weis, Management of acute myocardial infarction in patients presenting with persistent ST-segment elevation: the Task Force on the Management of ST-Segment Elevation Acute Myocardial Infarction of the European Society of Cardiology, European heart journal, 29 (2008) 2909-2945.

[5] G.W. Reed, J.E. Rossi, C.P. Cannon, Acute myocardial infarction, Lancet (London, England), 389 (2017) 197-210.

[6] H. Kumar, D.K. Choi, Hypoxia Inducible Factor Pathway and Physiological Adaptation: A Cell Survival Pathway?, Mediators Inflamm, 2015 (2015) 584758.

[7] E. Braunwald, The war against heart failure: the Lancet lecture, Lancet (London, England), 385 (2015) 812-824.

[8] K.I. Pinson, J. Brennan, S. Monkley, B.J. Avery, W.C. Skarnes, An LDL-receptor-related protein mediates Wnt signalling in mice, Nature, 407 (2000) 535-538.

[9] K. Tamai, M. Semenov, Y. Kato, R. Spokony, C. Liu, Y. Katsuyama, F. Hess, J.P. Saint-Jeannet, X. He, LDL-receptor-related proteins in Wnt signal transduction, Nature, 407 (2000) 530-535.

[10] M.V. Semenov, K. Tamai, B.K. Brott, M. Kuhl, S. Sokol, X. He, Head inducer Dickkopf-1 is a ligand for Wnt coreceptor LRP6, Current biology : CB, 11 (2001) 951-961.

[11] X. Li, Y. Zhang, H. Kang, W. Liu, P. Liu, J. Zhang, S.E. Harris, D. Wu, Sclerostin binds to LRP5/6 and antagonizes canonical Wnt signaling, The Journal of biological chemistry, 280 (2005) 19883-19887.

[12] J.C. Hsieh, L. Lee, L. Zhang, S. Wefer, K. Brown, C. DeRossi, M.E. Wines, T. Rosenquist, B.C. Holdener, Mesd encodes an LRP5/6 chaperone essential for specification of mouse embryonic polarity, Cell, 112 (2003) 355-367.

[13] X. Zeng, K. Tamai, B. Doble, S. Li, H. Huang, R. Habas, H. Okamura, J. Woodgett, X. He, A dual-kinase mechanism for Wnt co-receptor phosphorylation and activation, Nature, 438 (2005) 873-877.

[14] K. Tamai, X. Zeng, C. Liu, X. Zhang, Y. Harada, Z. Chang, X. He, A mechanism for Wnt coreceptor activation, Molecular cell, 13 (2004) 149-156.

[15] D.M. Joiner, J. Ke, Z. Zhong, H.E. Xu, B.O. Williams, LRP5 and LRP6 in development and disease, Trends Endocrinol Metab, 24 (2013) 31-39.

[16] L.M. Boyden, J. Mao, J. Belsky, L. Mitzner, A. Farhi, M.A. Mitnick, D. Wu, K. Insogna, R.P. Lifton, High bone density due to a mutation in LDL-receptor-related protein 5, The New England journal of medicine, 346 (2002) 1513-1521.

[17] K. Mi, G.V. Johnson, Role of the intracellular domains of LRP5 and LRP6 in activating the Wnt canonical pathway, J Cell Biochem, 95 (2005) 328-338.

[18] P.J. Hey, R.C. Twells, M.S. Phillips, N. Yusuke, S.D. Brown, Y. Kawaguchi, R. Cox, X. Guochun, V. Dugan, H. Hammond, M.L. Metzker, J.A. Todd, J.F.

Hess, Cloning of a novel member of the low-density lipoprotein receptor family, Gene, 216 (1998) 103-111.

[19] H. Clevers, R. Nusse, Wnt/beta-catenin signaling and disease, Cell, 149 (2012) 1192-1205.

[20] M. van Noort, J. Meeldijk, R. van der Zee, O. Destree, H. Clevers, Wnt signaling controls the phosphorylation status of beta-catenin, The Journal of biological chemistry, 277 (2002) 17901-17905.

[21] C. Liu, Y. Li, M. Semenov, C. Han, G.H. Baeg, Y. Tan, Z. Zhang, X. Lin, X. He, Control of beta-catenin phosphorylation/degradation by a dual-kinase mechanism, Cell, 108 (2002) 837-847.

[22] L. Agueda, R. Velazquez-Cruz, R. Urreizti, G. Yoskovitz, P. Sarrion, S. Jurado, R. Guerri, N. Garcia-Giralt, X. Nogues, L. Mellibovsky, A. Diez-Perez, P.J. Marie, S. Balcells, D. Grinberg, Functional relevance of the BMD-associated polymorphism rs312009: novel involvement of RUNX2 in LRP5 transcriptional regulation, Journal of bone and mineral research : the official journal of the American Society for Bone and Mineral Research, 26 (2011) 1133-1144.

[23] G. Holdsworth, S.J. Roberts, H.Z. Ke, Novel actions of sclerostin on bone, Journal of molecular endocrinology, 62 (2019) R167-r185.

[24] C.M. Laine, B.D. Chung, M. Susic, T. Prescott, O. Semler, T. Fiskerstrand, P. D'Eufemia, M. Castori, M. Pekkinen, E. Sochett, W.G. Cole, C. Netzer, O. Makitie, Novel mutations affecting LRP5 splicing in patients with osteoporosis-pseudoglioma syndrome (OPPG), Eur J Hum Genet, 19 (2011) 875-881.

[25] P. Bjorklund, J. Svedlund, A.K. Olsson, G. Akerstrom, G. Westin, The internally truncated LRP5 receptor presents a therapeutic target in breast cancer, PloS one, 4 (2009) e4243.

[26] Y. Li, W. Lu, X. He, A.L. Schwartz, G. Bu, LRP6 expression promotes cancer cell proliferation and tumorigenesis by altering beta-catenin subcellular distribution, Oncogene, 23 (2004) 9129-9135.

[27] M. Borrell-Pages, J.C. Romero, L. Badimon, LRP5 deficiency down-regulates Wnt signalling and promotes aortic lipid infiltration in hypercholesterolaemic mice, J Cell Mol Med, 19 (2015) 770-777.

[28] R.D. Little, J.P. Carulli, R.G. Del Mastro, J. Dupuis, M. Osborne, C. Folz, S.P. Manning, P.M. Swain, S.C. Zhao, B. Eustace, M.M. Lappe, L. Spitzer, S. Zweier, K. Braunschweiger, Y. Benchekroun, X. Hu, R. Adair, L. Chee, M.G. FitzGerald, C. Tulig, A. Caruso, N. Tzellas, A. Bawa, B. Franklin, S. McGuire, X. Nogues, G. Gong, K.M. Allen, A. Anisowicz, A.J. Morales, P.T. Lomedico, S.M. Recker, P. Van Eerdewegh, R.R. Recker, M.L. Johnson, A mutation in the LDL receptor-related protein 5 gene results in the autosomal dominant high-bone-mass trait, Am J Hum Genet, 70 (2002) 11-19.

[29] B.O. Williams, K.L. Insogna, Where Wnts went: the exploding field of Lrp5 and Lrp6 signaling in bone, Journal of bone and mineral research : the official journal of the American Society for Bone and Mineral Research, 24 (2009) 171-178.

[30] M. Kato, M.S. Patel, R. Levasseur, I. Lobov, B.H. Chang, D.A. Glass, 2nd, C. Hartmann, L. Li, T.H. Hwang, C.F. Brayton, R.A. Lang, G. Karsenty, L. Chan, Cbfa1-independent decrease in osteoblast proliferation, osteopenia, and persistent embryonic eye vascularization in mice deficient in Lrp5, a Wnt coreceptor, The Journal of cell biology, 157 (2002) 303-314.

[31] P. Babij, W. Zhao, C. Small, Y. Kharode, P.J. Yaworsky, M.L. Bouxsein, P.S. Reddy, P.V. Bodine, J.A. Robinson, B. Bhat, J. Marzolf, R.A. Moran, F. Bex, High bone mass in mice expressing a mutant LRP5 gene, Journal of bone

and mineral research : the official journal of the American Society for Bone and Mineral Research, 18 (2003) 960-974.

[32] V.K. Yadav, J.H. Ryu, N. Suda, K.F. Tanaka, J.A. Gingrich, G. Schutz, F.H. Glorieux, C.Y. Chiang, J.D. Zajac, K.L. Insogna, J.J. Mann, R. Hen, P. Ducy, G. Karsenty, Lrp5 controls bone formation by inhibiting serotonin synthesis in the duodenum, Cell, 135 (2008) 825-837.

[33] S.A. Rabbani, A. Arakelian, R. Farookhi, LRP5 knockdown: effect on prostate cancer invasion growth and skeletal metastasis in vitro and in vivo, Cancer medicine, 2 (2013) 625-635.

[34] B.H. Hoang, T. Kubo, J.H. Healey, R. Sowers, B. Mazza, R. Yang, A.G. Huvos, P.A. Meyers, R. Gorlick, Expression of LDL receptor-related protein 5 (LRP5) as a novel marker for disease progression in high-grade osteosarcoma, International journal of cancer, 109 (2004) 106-111.

[35] N.M. Badders, S. Goel, R.J. Clark, K.S. Klos, S. Kim, A. Bafico, C. Lindvall, B.O. Williams, C.M. Alexander, The Wnt receptor, Lrp5, is expressed by mouse mammary stem cells and is required to maintain the basal lineage, PloS one, 4 (2009) e6594.

[36] C. Lindvall, N.C. Evans, C.R. Zylstra, Y. Li, C.M. Alexander, B.O. Williams, The Wnt signaling receptor Lrp5 is required for mammary ductal stem cell activity and Wnt1-induced tumorigenesis, The Journal of biological chemistry, 281 (2006) 35081-35087.

[37] D.H. Kim, Y. Inagaki, T. Suzuki, R.X. Ioka, S.Z. Yoshioka, K. Magoori, M.J. Kang, Y. Cho, A.Z. Nakano, Q. Liu, T. Fujino, H. Suzuki, H. Sasano, T.T. Yamamoto, A new low density lipoprotein receptor related protein, LRP5, is expressed in hepatocytes and adrenal cortex, and recognizes apolipoprotein E, Journal of biochemistry, 124 (1998) 1072-1076.

[38] Z. Awan, M. Denis, D. Bailey, A. Giaid, A. Prat, D. Goltzman, N.G. Seidah, J. Genest, The LDLR deficient mouse as a model for aortic calcification and quantification by micro-computed tomography, Atherosclerosis, 219 (2011) 455-462.

[39] N.M. Rajamannan, The role of Lrp5/6 in cardiac valve disease: experimental hypercholesterolemia in the ApoE-/- /Lrp5-/- mice, J Cell Biochem, 112 (2011) 2987-2991.

[40] M. Borrell-Pages, J.C. Romero, L. Badimon, Cholesterol modulates LRP5 expression in the vessel wall, Atherosclerosis, 235 (2014) 363-370.

[41] T. Fujino, H. Asaba, M.J. Kang, Y. Ikeda, H. Sone, S. Takada, D.H. Kim, R.X. Ioka, M. Ono, H. Tomoyori, M. Okubo, T. Murase, A. Kamataki, J. Yamamoto, K. Magoori, S. Takahashi, Y. Miyamoto, H. Oishi, M. Nose, M. Okazaki, S. Usui, K. Imaizumi, M. Yanagisawa, J. Sakai, T.T. Yamamoto, Low-density lipoprotein receptor-related protein 5 (LRP5) is essential for normal cholesterol metabolism and glucose-induced insulin secretion, Proceedings of the National Academy of Sciences of the United States of America, 100 (2003) 229-234.

[42] K. Magoori, M.J. Kang, M.R. Ito, H. Kakuuchi, R.X. Ioka, A. Kamataki, D.H. Kim, H. Asaba, S. Iwasaki, Y.A. Takei, M. Sasaki, S. Usui, M. Okazaki, S. Takahashi, M. Ono, M. Nose, J. Sakai, T. Fujino, T.T. Yamamoto, Severe hypercholesterolemia, impaired fat tolerance, and advanced atherosclerosis in mice lacking both low density lipoprotein receptor-related protein 5 and apolipoprotein E, The Journal of biological chemistry, 278 (2003) 11331-11336.

[43] G.L. Semenza, HIF-1 and mechanisms of hypoxia sensing, Curr Opin Cell Biol, 13 (2001) 167-171.

[44] D.A. Chan, P.D. Sutphin, S.E. Yen, A.J. Giaccia, Coordinate regulation of the oxygen-dependent degradation domains of hypoxia-inducible factor 1 alpha, Molecular and cellular biology, 25 (2005) 6415-6426.

[45] B.H. Jiang, E. Rue, G.L. Wang, R. Roe, G.L. Semenza, Dimerization, DNA binding, and transactivation properties of hypoxia-inducible factor 1, The Journal of biological chemistry, 271 (1996) 17771-17778.

[46] B.H. Jiang, J.Z. Zheng, S.W. Leung, R. Roe, G.L. Semenza, Transactivation and inhibitory domains of hypoxia-inducible factor 1alpha. Modulation of transcriptional activity by oxygen tension, The Journal of biological chemistry, 272 (1997) 19253-19260.

[47] R.S. Freeman, D.M. Hasbani, E.A. Lipscomb, J.A. Straub, L. Xie, SM-20, EGL-9, and the EGLN family of hypoxia-inducible factor prolyl hydroxylases, Mol Cells, 16 (2003) 1-12.

[48] A. Ozer, L.C. Wu, R.K. Bruick, The candidate tumor suppressor ING4 represses activation of the hypoxia inducible factor (HIF), Proceedings of the National Academy of Sciences of the United States of America, 102 (2005) 7481-7486.

[49] L.E. Huang, Z. Arany, D.M. Livingston, H.F. Bunn, Activation of hypoxia-inducible transcription factor depends primarily upon redox-sensitive stabilization of its alpha subunit, The Journal of biological chemistry, 271 (1996) 32253-32259.

[50] E. Berra, E. Benizri, A. Ginouves, V. Volmat, D. Roux, J. Pouyssegur, HIF prolyl-hydroxylase 2 is the key oxygen sensor setting low steady-state levels of HIF-1alpha in normoxia, Embo j, 22 (2003) 4082-4090.

[51] C.J. Schofield, P.J. Ratcliffe, Oxygen sensing by HIF hydroxylases, Nat Rev Mol Cell Biol, 5 (2004) 343-354.

[52] D. Escuin, E.R. Kline, P. Giannakakou, Both microtubule-stabilizing and microtubule-destabilizing drugs inhibit hypoxia-inducible factor-1alpha accumulation and activity by disrupting microtubule function, Cancer Res, 65 (2005) 9021-9028.

[53] R.J. Appelhoff, Y.M. Tian, R.R. Raval, H. Turley, A.L. Harris, C.W. Pugh, P.J. Ratcliffe, J.M. Gleadle, Differential function of the prolyl hydroxylases PHD1, PHD2, and PHD3 in the regulation of hypoxia-inducible factor, The Journal of biological chemistry, 279 (2004) 38458-38465.

[54] E.J. Soilleux, H. Turley, Y.M. Tian, C.W. Pugh, K.C. Gatter, A.L. Harris, Use of novel monoclonal antibodies to determine the expression and distribution of the hypoxia regulatory factors PHD-1, PHD-2, PHD-3 and FIH in normal and neoplastic human tissues, Histopathology, 47 (2005) 602-610.

[55] J. Huang, Q. Zhao, S.M. Mooney, F.S. Lee, Sequence determinants in hypoxia-inducible factor-1alpha for hydroxylation by the prolyl hydroxylases PHD1, PHD2, and PHD3, The Journal of biological chemistry, 277 (2002) 39792-39800.

[56] E. Metzen, U. Berchner-Pfannschmidt, P. Stengel, J.H. Marxsen, I. Stolze, M. Klinger, W.Q. Huang, C. Wotzlaw, T. Hellwig-Burgel, W. Jelkmann, H. Acker, J. Fandrey, Intracellular localisation of human HIF-1 alpha hydroxylases: implications for oxygen sensing, Journal of cell science, 116 (2003) 1319-1326.

[57] Z. Khan, G.K. Michalopoulos, D.B. Stolz, Peroxisomal localization of hypoxia-inducible factors and hypoxia-inducible factor regulatory hydroxylases in primary rat hepatocytes exposed to hypoxia-reoxygenation, The American journal of pathology, 169 (2006) 1251-1269.

[58] E. Metzen, D.P. Stiehl, K. Doege, J.H. Marxsen, T. Hellwig-Burgel, W. Jelkmann, Regulation of the prolyl hydroxylase domain protein 2 (phd2/egln-1)

gene: identification of a functional hypoxia-responsive element, The Biochemical journal, 387 (2005) 711-717.

[59] J.H. Marxsen, P. Stengel, K. Doege, P. Heikkinen, T. Jokilehto, T. Wagner, W. Jelkmann, P. Jaakkola, E. Metzen, Hypoxia-inducible factor-1 (HIF-1) promotes its degradation by induction of HIF-alpha-prolyl-4-hydroxylases, The Biochemical journal, 381 (2004) 761-767.

[60] D.P. Stiehl, R. Wirthner, J. Koditz, P. Spielmann, G. Camenisch, R.H. Wenger, Increased prolyl 4-hydroxylase domain proteins compensate for decreased oxygen levels. Evidence for an autoregulatory oxygen-sensing system, The Journal of biological chemistry, 281 (2006) 23482-23491.

[61] K.O. Choi, T. Lee, N. Lee, J.H. Kim, E.G. Yang, J.M. Yoon, J.H. Kim, T.G. Lee, H. Park, Inhibition of the catalytic activity of hypoxia-inducible factor-1alpha-prolyl-hydroxylase 2 by a MYND-type zinc finger, Molecular pharmacology, 68 (2005) 1803-1809.

[62] R. Natarajan, F.N. Salloum, B.J. Fisher, R.C. Kukreja, A.A. Fowler, 3rd, Hypoxia inducible factor-1 activation by prolyl 4-hydroxylase-2 gene silencing attenuates myocardial ischemia reperfusion injury, Circulation research, 98 (2006) 133-140.

[63] R. Ockaili, R. Natarajan, F. Salloum, B.J. Fisher, D. Jones, A.A. Fowler, 3rd, R.C. Kukreja, HIF-1 activation attenuates postischemic myocardial injury: role for heme oxygenase-1 in modulating microvascular chemokine generation, American journal of physiology. Heart and circulatory physiology, 289 (2005) H542-548.

[64] M.P. Alfaro, M. Pagni, A. Vincent, J. Atkinson, M.F. Hill, J. Cates, J.M. Davidson, J. Rottman, E. Lee, P.P. Young, The Wnt modulator sFRP2 enhances mesenchymal stem cell engraftment, granulation tissue formation and myocardial

repair, Proceedings of the National Academy of Sciences of the United States of America, 105 (2008) 18366-18371.

[65] L. Barandon, F. Casassus, L. Leroux, C. Moreau, C. Allieres, J.M. Lamaziere, P. Dufourcq, T. Couffinhal, C. Duplaa, Secreted frizzled-related protein-1 improves postinfarction scar formation through a modulation of inflammatory response, Arterioscler Thromb Vasc Biol, 31 (2011) e80-87.

[66] Z. Zhang, A. Deb, Z. Zhang, A. Pachori, W. He, J. Guo, R. Pratt, V.J. Dzau, Secreted frizzled related protein 2 protects cells from apoptosis by blocking the effect of canonical Wnt3a, J Mol Cell Cardiol, 46 (2009) 370-377.

[67] S. Saraswati, M.P. Alfaro, C.A. Thorne, J. Atkinson, E. Lee, P.P. Young, Pyrvinium, a potent small molecule Wnt inhibitor, promotes wound repair and post-MI cardiac remodeling, PloS one, 5 (2010) e15521.

[68] D. Wo, J. Peng, D.N. Ren, L. Qiu, J. Chen, Y. Zhu, Y. Yan, H. Yan, J. Wu, E. Ma, T.P. Zhong, Y. Chen, Z. Liu, S. Liu, L. Ao, Z. Liu, C. Jiang, J. Peng, Y. Zou, Q. Qian, W. Zhu, Opposing Roles of Wnt Inhibitors IGFBP-4 and Dkk1 in Cardiac Ischemia by Differential Targeting of LRP5/6 and beta-catenin, Circulation, 134 (2016) 1991-2007.

[69] T. Abe, P. Zhou, K. Jackman, C. Capone, B. Casolla, K. Hochrainer, T. Kahles, M.E. Ross, J. Anrather, C. Iadecola, Lipoprotein receptor-related protein-6 protects the brain from ischemic injury, Stroke, 44 (2013) 2284-2291.

[70] M. Borrell-Pages, G. Vilahur, J.C. Romero, L. Casani, M.T. Bejar, L. Badimon, LRP5/canonical Wnt signalling and healing of ischemic myocardium, 111 (2016) 67.

[71] B.T. MacDonald, M.V. Semenov, H. Huang, X. He, Dissecting molecular differences between Wnt coreceptors LRP5 and LRP6, PloS one, 6 (2011) e23537.

[72] B.T. MacDonald, K. Tamai, X. He, Wnt/beta-catenin signaling: components, mechanisms, and diseases, Dev Cell, 17 (2009) 9-26.

[73] E.N. Chin, J.A. Martin, S. Kim, S.A. Fakhraldeen, C.M. Alexander, Lrp5 Has a Wnt-Independent Role in Glucose Uptake and Growth for Mammary Epithelial Cells, Molecular and cellular biology, 36 (2015) 871-885.

[74] J. Li, C. Li, D. Liang, F. Lv, T. Yuan, E. The, X. Ma, Y. Wu, L. Zhen, D. Xie, S. Wang, Y. Liu, J. Huang, J. Shi, Y. Liu, D. Shi, L. Xu, L. Lin, L. Peng, J. Cui, W. Zhu, Y.H. Chen, LRP6 acts as a scaffold protein in cardiac gap junction assembly, Nat Commun, 7 (2016) 11775.

[75] H. Song, M.J. Cha, B.W. Song, I.K. Kim, W. Chang, S. Lim, E.J. Choi, O. Ham, S.Y. Lee, N. Chung, Y. Jang, K.C. Hwang, Reactive oxygen species inhibit adhesion of mesenchymal stem cells implanted into ischemic myocardium via interference of focal adhesion complex, Stem Cells, 28 (2010) 555-563.

[76] H. Song, H.J. Hwang, W. Chang, B.W. Song, M.J. Cha, I.K. Kim, S. Lim, E.J. Choi, O. Ham, C.Y. Lee, J.H. Park, S.Y. Lee, E. Choi, C. Lee, M. Lee, M.H. Lee, S.H. Kim, Y. Jang, K.C. Hwang, Cardiomyocytes from phorbol myristate acetate-activated mesenchymal stem cells restore electromechanical function in infarcted rat hearts, Proceedings of the National Academy of Sciences of the United States of America, 108 (2011) 296-301.

[77] S. Adachi, H. Ito, M. Tamamori-Adachi, Y. Ono, T. Nozato, S. Abe, M. Ikeda, F. Marumo, M. Hiroe, Cyclin A/cdk2 activation is involved in hypoxia-induced apoptosis in cardiomyocytes, Circulation research, 88 (2001) 408-414.

[78] D. Villar, A. Vara-Vega, M.O. Landazuri, L. Del Peso, Identification of a region on hypoxia-inducible-factor prolyl 4-hydroxylases that determines their specificity for the oxygen degradation domains, The Biochemical journal, 408 (2007) 231-240.

[79] E. Murphy, C. Steenbergen, Mechanisms underlying acute protection from cardiac ischemia-reperfusion injury, Physiol Rev, 88 (2008) 581-609.

[80] S.L. Holmen, T.A. Giambernardi, C.R. Zylstra, B.D. Buckner-Berghuis, J.H. Resau, J.F. Hess, V. Glatt, M.L. Bouxsein, M. Ai, M.L. Warman, B.O. Williams, Decreased BMD and limb deformities in mice carrying mutations in both Lrp5 and Lrp6, Journal of bone and mineral research : the official journal of the American Society for Bone and Mineral Research, 19 (2004) 2033-2040.

[81] Z. Zhong, J.J. Baker, C.R. Zylstra-Diegel, B.O. Williams, Lrp5 and Lrp6 play compensatory roles in mouse intestinal development, J Cell Biochem, 113 (2012) 31-38.

[82] O.G. Kelly, K.I. Pinson, W.C. Skarnes, The Wnt co-receptors Lrp5 and Lrp6 are essential for gastrulation in mice, Development, 131 (2004) 2803-2815.

[83] S.L. Holmen, A. Salic, C.R. Zylstra, M.W. Kirschner, B.O. Williams, A novel set of Wnt-Frizzled fusion proteins identifies receptor components that activate beta -catenin-dependent signaling, The Journal of biological chemistry, 277 (2002) 34727-34735.

[84] L.C. Zelarayan, C. Noack, B. Sekkali, J. Kmecova, C. Gehrke, A. Renger, M.P. Zafiriou, R. van der Nagel, R. Dietz, L.J. de Windt, J.L. Balligand, M.W. Bergmann, Beta-Catenin downregulation attenuates ischemic cardiac remodeling through enhanced resident precursor cell differentiation, Proceedings of the National Academy of Sciences of the United States of America, 105 (2008) 19762-19767.

[85] V.A. van de Schans, S.W. van den Borne, A.E. Strzelecka, B.J. Janssen, J.L. van der Velden, R.C. Langen, A. Wynshaw-Boris, J.F. Smits, W.M. Blankesteijn, Interruption of Wnt signaling attenuates the onset of pressure overload-induced cardiac hypertrophy, Hypertension, 49 (2007) 473-480.

[86] K.C. Woulfe, E. Gao, H. Lal, D. Harris, Q. Fan, R. Vagnozzi, M. DeCaul, X. Shang, S. Patel, J.R. Woodgett, T. Force, J. Zhou, Glycogen synthase kinase-3beta regulates post-myocardial infarction remodeling and stress-induced cardiomyocyte proliferation in vivo, Circulation research, 106 (2010) 1635-1645.

[87] M.I. Oerlemans, M.J. Goumans, B. van Middelaar, H. Clevers, P.A. Doevendans, J.P. Sluijter, Active Wnt signaling in response to cardiac injury, Basic research in cardiology, 105 (2010) 631-641.

[88] F.J. Staal, T.C. Luis, M.M. Tiemessen, WNT signalling in the immune system: WNT is spreading its wings, Nature reviews. Immunology, 8 (2008) 581-593.